Electronic Supplementary Material (ESI) for ChemComm.

Isolation and Characterization of a High-Spin Mixed-Valent Iron Dinitrogen Complex

Sean F. McWilliams, Philip C. Bunting, Venkatesan Kathiresan, Brandon Q. Mercado, Brian M. Hoffman, Jeffrey R. Long and Patrick L. Holland*

Table of Contents

Experimental

General

All manipulations were performed under a nitrogen atmosphere (or argon atmosphere where specified) by Schlenk techniques or in an M. Braun glovebox maintained at or below 1 ppm of O_2. Glassware was oven-dried at 150 °C for at least 12 h before use. Graphite, Celite, and 4 Å molecular sieves were dried at 200 °C under vacuum for at least 12 h. Pentane, hexane, and diethyl ether were purified by passage through activated alumina and Q5 columns from Glass Contour Co, under Ar. THF was distilled under Ar from a potassium benzophenone ketyl solution. All solvents were stored over 4 Å molecular sieves and passed through a plug of activated alumina immediately prior to use. Benzene-d_6 was dried over activated alumina and stored over 4 Å molecular sieves. THF-d_8 was vacuum transferred from sodium benzophenone ketyl solutions and was stored over 4 Å molecular sieves. $^{15}N_2$ (98%) was purchased from Cambridge Isotope Laboratories. Potassium was obtained from Sigma-Aldrich (98%). Potassium on graphite was prepared by heating stoichiometric amounts of potassium and graphite at 140 °C under an argon atmosphere.[1] 18-crown-6 (ACROS Organics) was dried over 4 Å molecular sieves as a solution in diethyl ether and then volatiles removed under vacuum prior to use. $[L^{Me}Fe(\mu\text{-}N_2)FeL^{Me}]$ (**1**),[2] $K_2[L^{Me}Fe(\mu\text{-}N_2)FeL^{Me}]$ (**4**),[2] $[L^{tBu}Fe(\mu\text{-}N_2)FeL^{tBu}]$,[3] and $K_2[L^{Me}Fe(\mu\text{-}N_2)FeL^{Me}]$[3] were prepared according to the previously reported procedure. NMR data were collected on an Agilent 400 or 500 MHz spectrometer. Chemical shifts in ^1H NMR spectra are referenced to external $SiMe_4$ using the residual protiated solvent peaks as internal standards: C_6D_5H (δ 7.16 ppm), $C_6D_{11}H$ (δ 1.38 ppm), and THF-d_8 (δ 3.58 ppm). Solution magnetic susceptibilities were determined by the Evans method.[4] Elemental analyses were performed at the CENTC Elemental Analysis Facility at the University of Rochester. IR spectra were collected on an Alpha Platinum ATR IR Spectrometer. UV-vis spectra were recorded on a Cary 50 spectrometer using Schlenk-adapted quartz cuvettes with a 1, 2, or 10 mm path length with a Unisoku CoolSpek UV USP-203A cryostat.

^{57}Fe Mössbauer Spectroscopy. Solid & frozen solution Mössbauer samples were packed in Delrin sample cups and loaded into the spectrometer at 77 K. Mössbauer measurements were performed using a SEE Co. MS4 Mössbauer spectrometer integrated with a Janis SVT-400T He/N_2 cryostat for measurements at 80 K with a 0.07 T applied magnetic field. Isomer shifts were determined relative to α-iron at 298 K. All Mössbauer spectra were fit using the program WMoss (SEE Co.), using Lorentzian doublets.

SQUID Magnetometry. All magnetic measurements were carried out in a Quantum Design MPMS-XL SQUID Magnetometer. Polycrystalline samples were loaded into quartz tubes with an equal amount of eicosane in a glovebox. A sealable hose adapter was attached to the tubes so they could be sealed under vacuum. The eicosane was melted around the sample to restrain the crystallites. Samples were measured from 1.7 to 300 K at DC fields ranging from 0 to 7 T. AC magnetic susceptibility from the MPMS was collected using a 4 Oe probe field. All data were corrected for diamagnetic contributions of the eicosane and the sample itself using Pascal's constants.

The ac susceptometry data were fit using a generalized Debye model that accounts for relaxation time (τ), isothermal susceptibility (χ_T), adiabatic susceptibility (χ_S), and the presence of a distribution of relaxation times (α).[5]

Low-temperature reduced magnetization were fit using the freely available program, PHI,[6] and the zero-field splitting Hamiltonian:

$$H_{ZFS} = D\left[S_z^2 - \frac{1}{3}S(S+1)\right] + E\left[S_x^2 - S_y^2\right] + g_{\parallel}\mu_B H S_z + g_{\perp}\mu_B H S_x$$

Synthesis and characterization:

Synthesis of [$L^{Me}Fe(\mu\text{-}N_2)FeL^{Me}$][K(18-crown-6)$(THF)_2$]THF (2). $L^{Me}Fe(\mu\text{-}N_2)FeL^{Me}$ (97.7 mg, 0.100 mmol) and 18-crown-6 (32.1 mg, 0.122 mmol) were dissolved in THF (6 mL) yielding a dark purple solution. Potassium graphite (KC_8, 14.7 mg, 0.109 mmol) was added to the stirring purple solution resulting in a color change to dark green upon mixing. The reaction was allowed to stir for 1 h. Volatile materials were removed under vacuum and resulting dark solid was washed with diethyl ether (10 mL). The solid was extracted with THF (3 mL) and filtered through Celite to give a dark green solution. Pentane (10 mL) was added to the THF filtrate resulting in dark precipitate. The precipitate was collected on a fine frit and washed with diethyl ether (5 mL) and toluene (5 mL). The solid was dried under vacuum yielding dark green **2** (94.3 mg, 63%). Single crystals of **2** for X-ray diffraction (XRD) were obtained using a THF/pentane vapor diffusion at −40 °C for 2 d. ^{1}H NMR (400 MHz, THF-d_8, 298 K): δ 18 (8H, *m*-**H** or -C**H**$(CH_3)_2$), 3 (24H, 18-crown-6), −1 (24H, -CH(C**H**$_3)_2$, −16 (6H), -26 (24H, -CH(C**H**$_3)_2$), −48 (4H, *p*-**H**), −53 (2H, backbone -C**H**), -319 (8H, *m*-**H** or -C**H**$(CH_3)_2$). μ_{eff} (Evans, THF-d_8, 298 K) = 6.6(1) B.M. IR (ATR, neat): 3046 (w), 3013 (w), 2952 (m), 2901 (m), 2862 (m), 1747 (w, br), 1584 (w), 1506 (m), 1456 (m), 1433 (m), 1386 (s), 1351 (m), 1317 (s), 1300 (m), 1247 (m), 1172 (m), 1099 (s), 1054 (m), 1021 (m), 964 (s), 933 (w), 884 (m), 833 (m), 797 (m), 750 (m), 707 (w), 630 (w), 536 (w), 438 (w). UV-vis (THF, 295 K, ε in $mM^{-1}cm^{-1}$): 369 (21), 702 (13), 891 (4.5) nm. Anal. Calcd for $C_{82}H_{130}N_6O_9Fe_2K$: C, 65.89; H, 8.77; N, 5.62. Found: C, 65.91; H, 8.67; N, 5.97. Mössbauer (80 K, solid): Alternating Fit: δ_1 = 0.49(2) mm s^{-1}, $|\Delta E_Q|$ = 1.71(2) mm s^{-1}, Γ = 0.37 mm s^{-1}, Rel. Area = 0.50; : δ_2 = 0.63(2) mm s^{-1}, $|\Delta E_Q|$ = 1.75(2) mm s^{-1}, Γ = 0.47 mm s^{-1}, Rel. Area = 0.50. Nested Fit: δ_1 = 0.54(2) mm s^{-1}, $|\Delta E_Q|$ = 1.61(2) mm s^{-1}, Γ = 0.38 mm s^{-1}, Rel. Area = 0.50; : δ_2 = 0.55(2) mm s^{-1}, $|\Delta E_Q|$ = 1.87(2) mm s^{-1}, Γ = 0.46 mm s^{-1}, Rel. Area = 0.50.

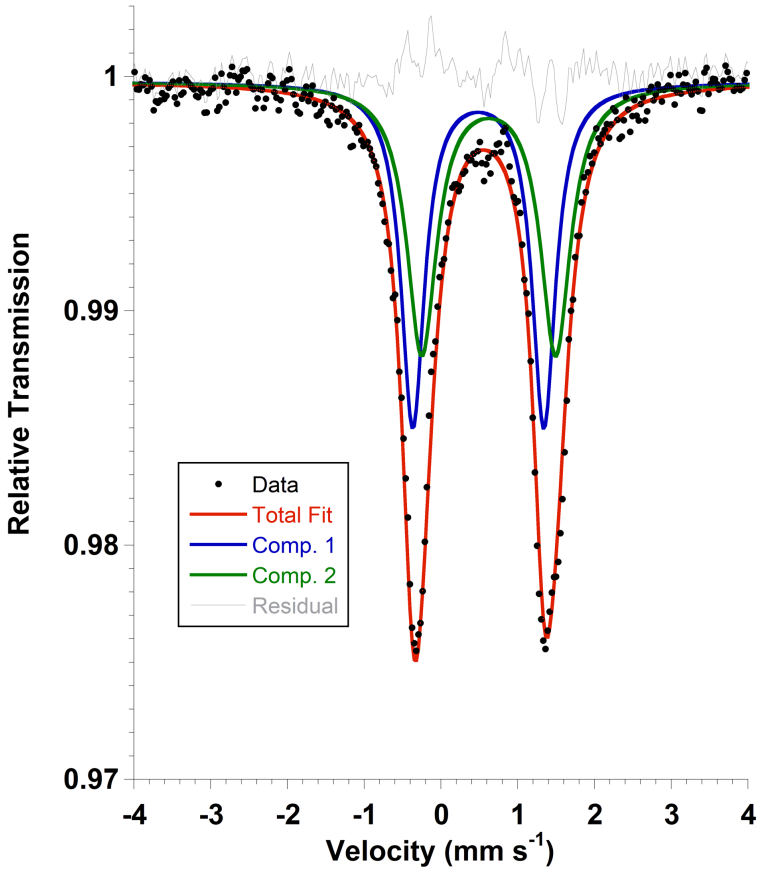

Figure S-1. Zero-field Mössbauer spectrum of solid [$L^{Me}Fe(\mu\text{-}N_2)FeL^{Me}$][K(18-crown-6)$(THF)_2$] (**2**) recorded at 80 K. This figure shows the staggered fit where the black circles represent the data, the red line is a two component simulation. The blue line represents a component with parameters δ = 0.49(2) mm/s, $|\Delta E_Q|$ = 1.71(2) mm/s, Γ = 0.37, and relative area = 0.50. The green line represents a second component with δ = 0.63(2) mm/s, $|\Delta E_Q|$ = 1.75(2) mm/s, Γ = 0.47, relative area = 0.50, and the gray line is the residual.

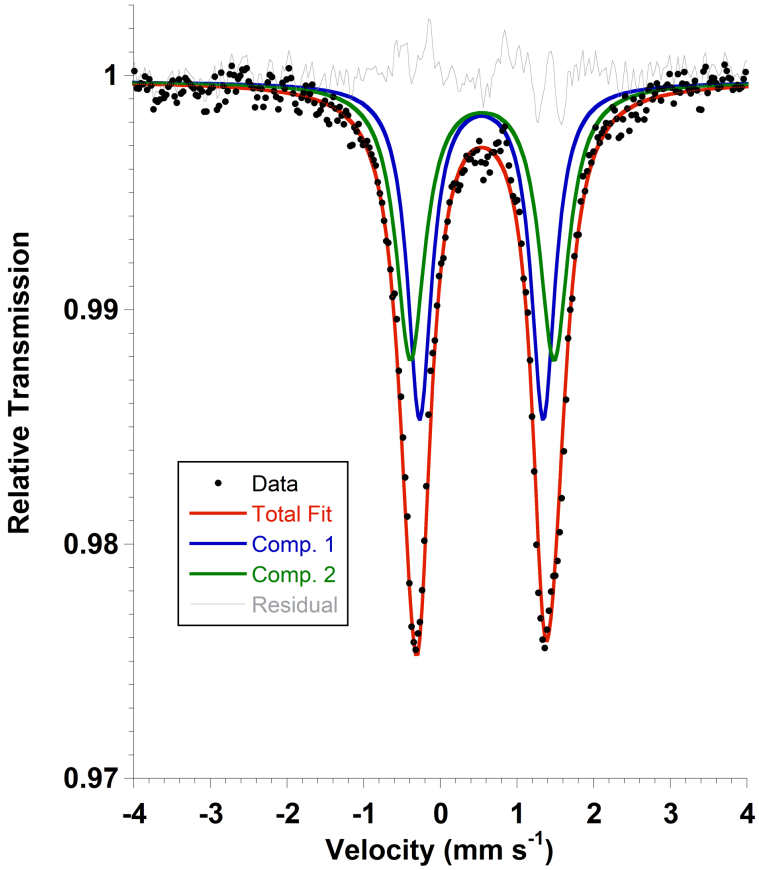

Figure S-2. Zero-field Mössbauer spectrum of solid [$L^{Me}Fe(\mu\text{-}N_2)FeL^{Me}$][K(18-crown-6)$(THF)_2$] (**2**) recorded at 80 K. This figure shows an alternative nested fit where the black circles represent the data, the red line is a two component simulation. The blue line represents a component with parameters δ = 0.54(2) mm/s, $|\Delta E_Q|$ = 1.61(2) mm/s, Γ = 0.38, and relative area = 0.50. The green line represents a second component with δ = 0.55(2) mm/s, $|\Delta E_Q|$ = 1.87(2) mm/s, Γ = 0.46, relative area = 0.50, and the gray line is the residual.

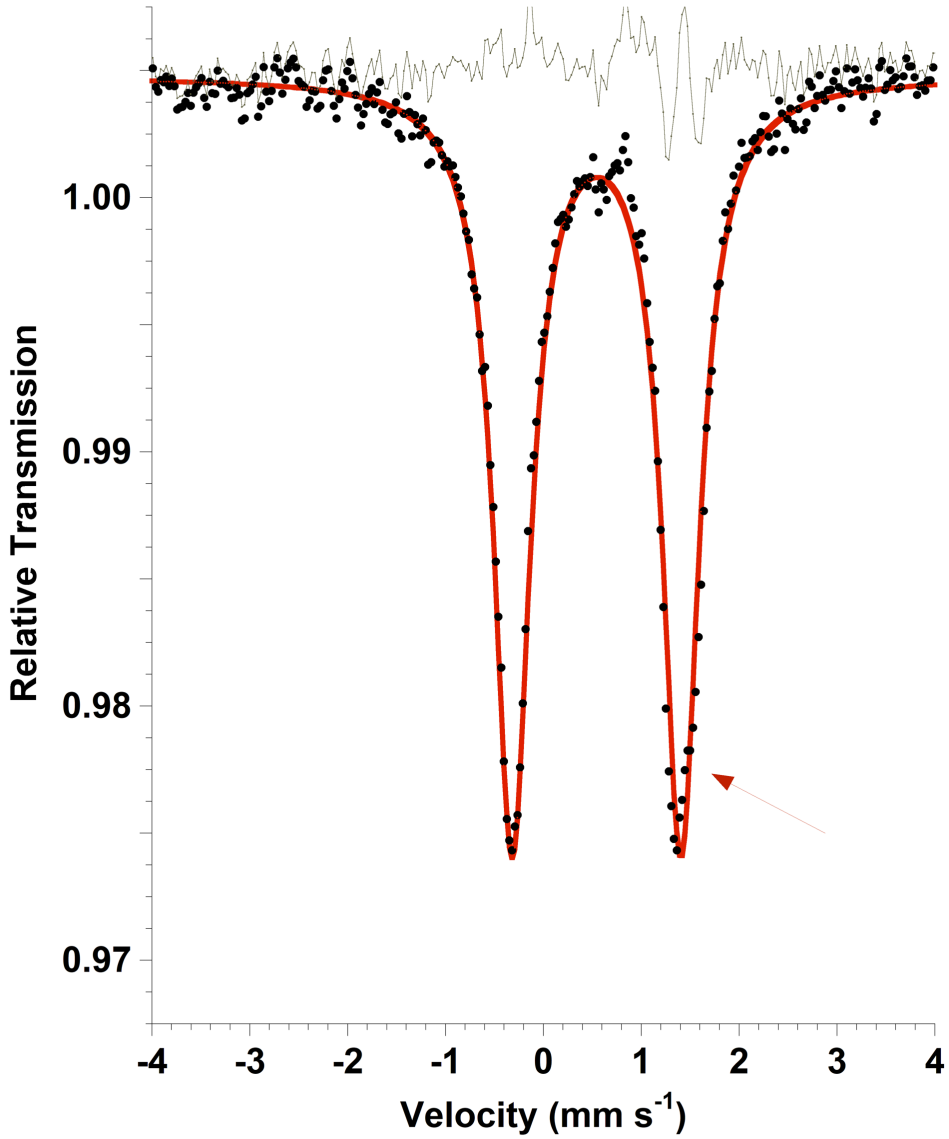

Figure S-3. Zero-field Mössbauer spectrum of solid [$L^{Me}Fe(\mu\text{-}N_2)FeL^{Me}$][K(18-crown-6)$(THF)_2$] (**2**) recorded at 80 K. This figure shows an alternative single component fit where the black circles represent the data, the red line is a one component simulation with parameters δ = 0.54(2) mm/s, $|\Delta E_Q|$ = 1.73(2) mm/s, and Γ = 0.46 mm/s. The red arrow highlights an imperfection in the line shape indicative of more than one component, which gives a large signal in the residual.

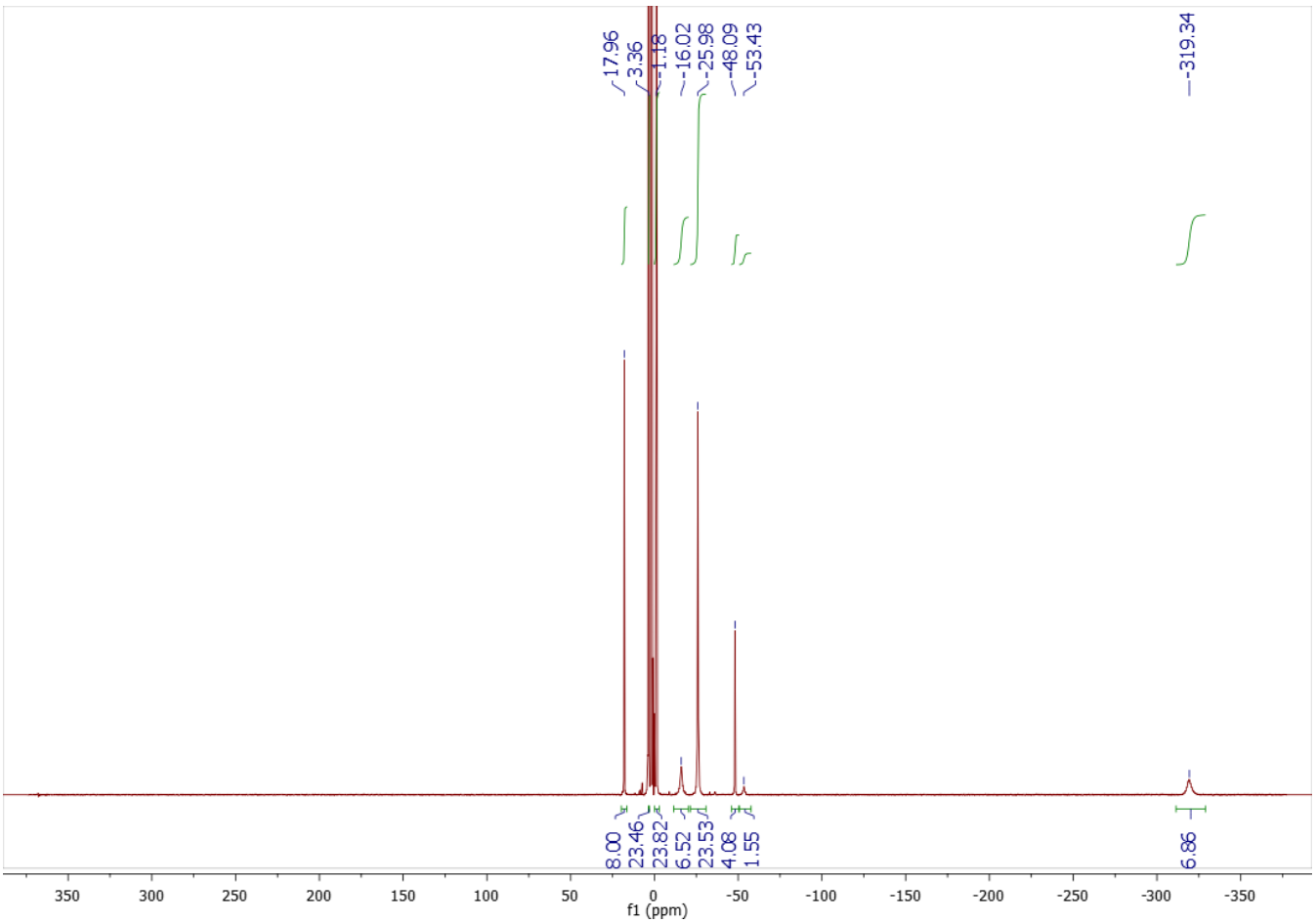

Figure S-4. ^{1}H NMR spectrum of [L^{Me}Fe(μ-N_2)FeL^{Me}][K(18-crown-6)(THF)$_2$] (**2**) in THF-d_8.

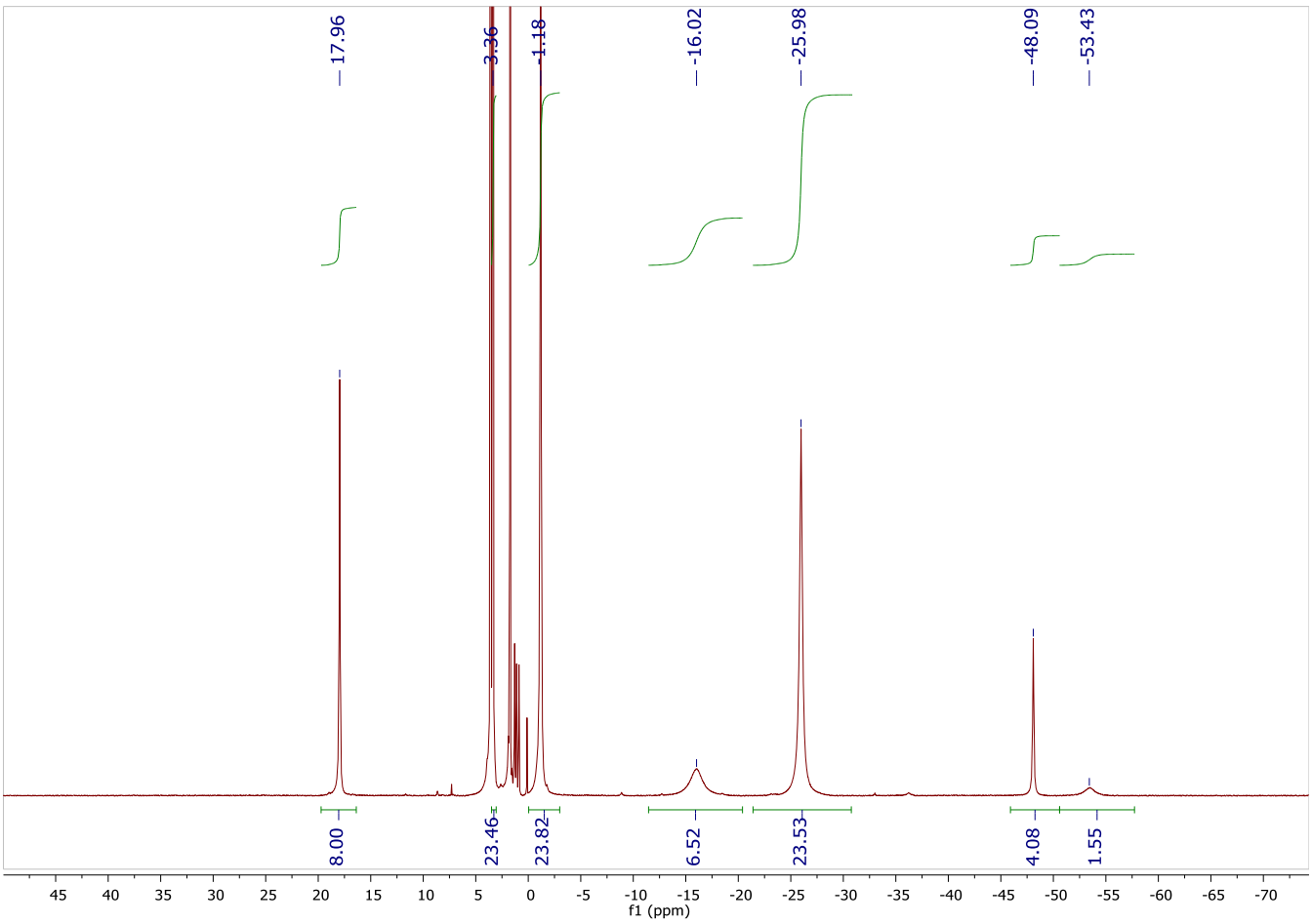

Figure S-5. Zoomed in ^{1}H NMR spectrum between +50 and -80 ppm of [$L^{Me}Fe(\mu\text{-}N_2)FeL^{Me}$][K(18-crown-6)$(THF)_2$] (**2**) in THF-$d_8$.

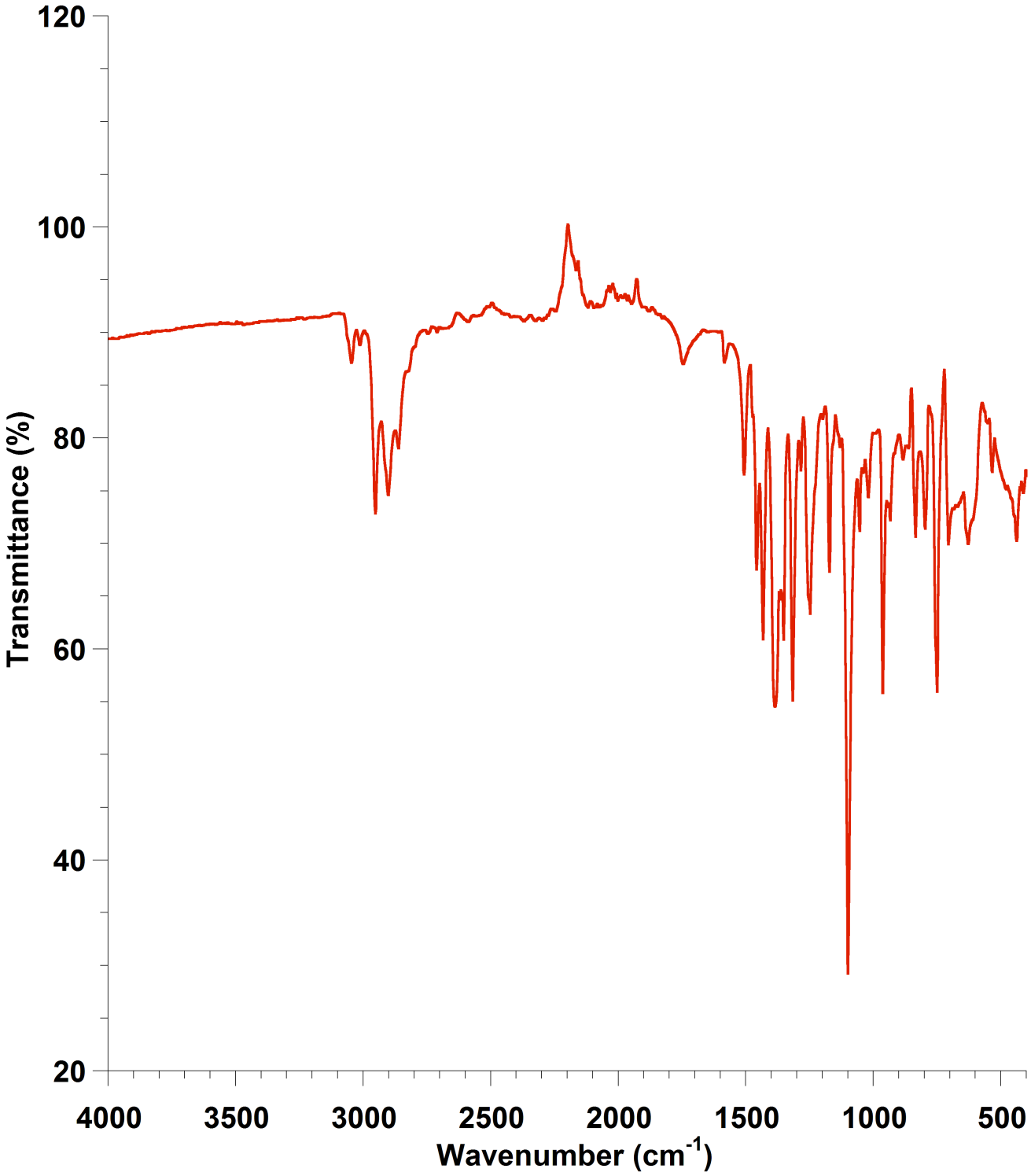

Figure S-6. IR spectrum (ATR) of solid [$L^{Me}Fe(\mu\text{-}N_2)FeL^{Me}$][K(18-crown-6)$(THF)_2$] (**2**) crystallized under natural abundance N_2.

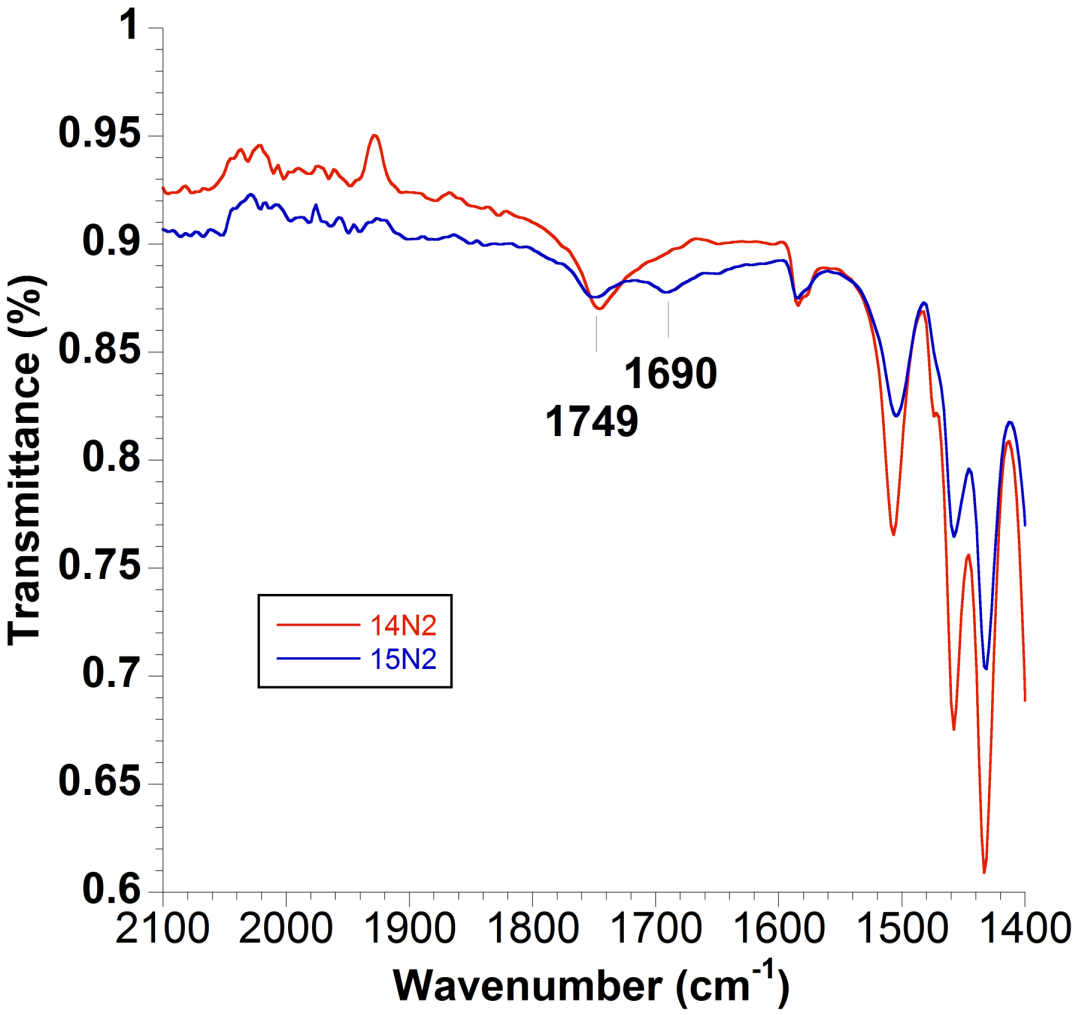

Figure S-7. IR spectrum (ATR) of solid [$L^{Me}Fe(\mu\text{-}N_2)FeL^{Me}$][K(18-crown-6)$(THF)_2$] (**2**) crystallized under natural abundance N_2 (red) and $^{15}N_2$ (blue). There is a minor peak at the ^{14}N value, presumably from contamination with natural abundance nitrogen.

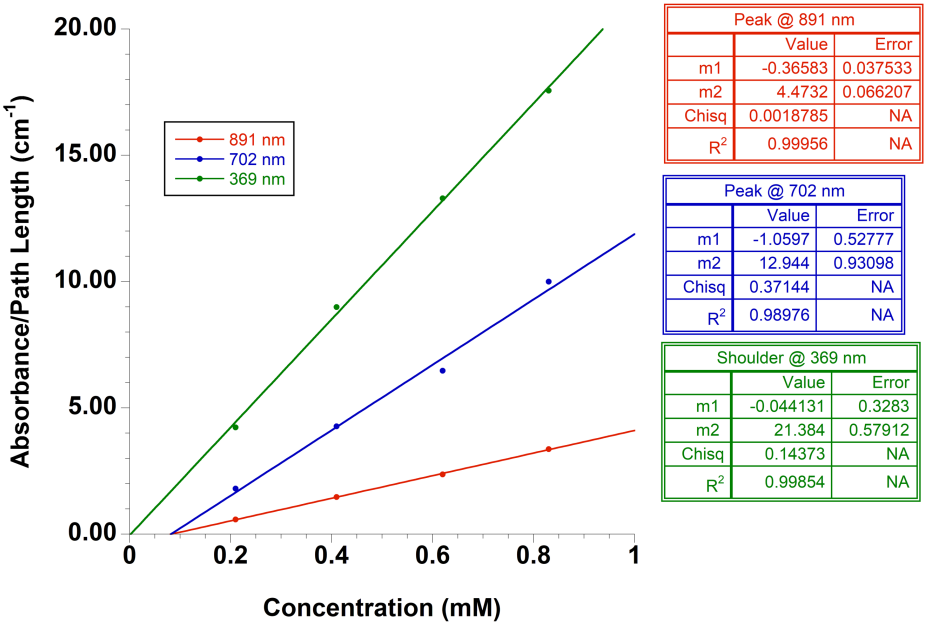

Peak @ 891 nm		
	Value	Error
m1	-0.36583	0.037533
m2	4.4732	0.066207
Chisq	0.0018785	NA
R^2	0.99956	NA

Peak @ 702 nm		
	Value	Error
m1	-1.0597	0.52777
m2	12.944	0.93098
Chisq	0.37144	NA
R^2	0.98976	NA

Shoulder @ 369 nm		
	Value	Error
m1	-0.044131	0.3283
m2	21.384	0.57912
Chisq	0.14373	NA
R^2	0.99854	NA

Figure S-8: Beer-Lambert Law plot of selected UV-vis spectral features for [$L^{Me}Fe(\mu\text{-}N_2)FeL^{Me}$][K(18-crown-6)$(THF)_2$] (**2**) in THF solutions. Trendline equations are in the boxes to the right.

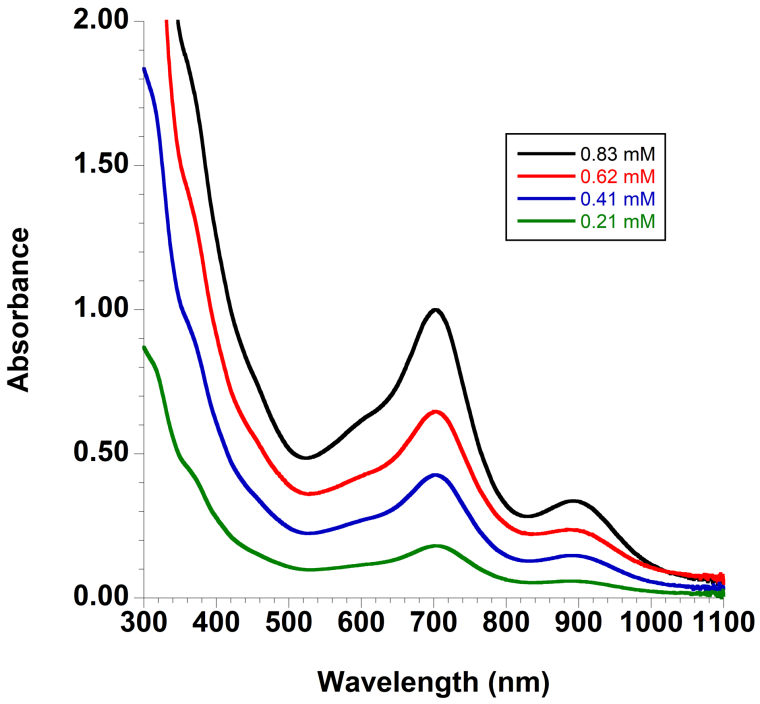

Figure S-9: UV-visible spectra of [$L^{Me}Fe(\mu\text{-}N_2)FeL^{Me}$][K(18-crown-6)$(THF)_2$] (**2**) in THF solutions at concentrations from 0.21 to 0.83 mM.

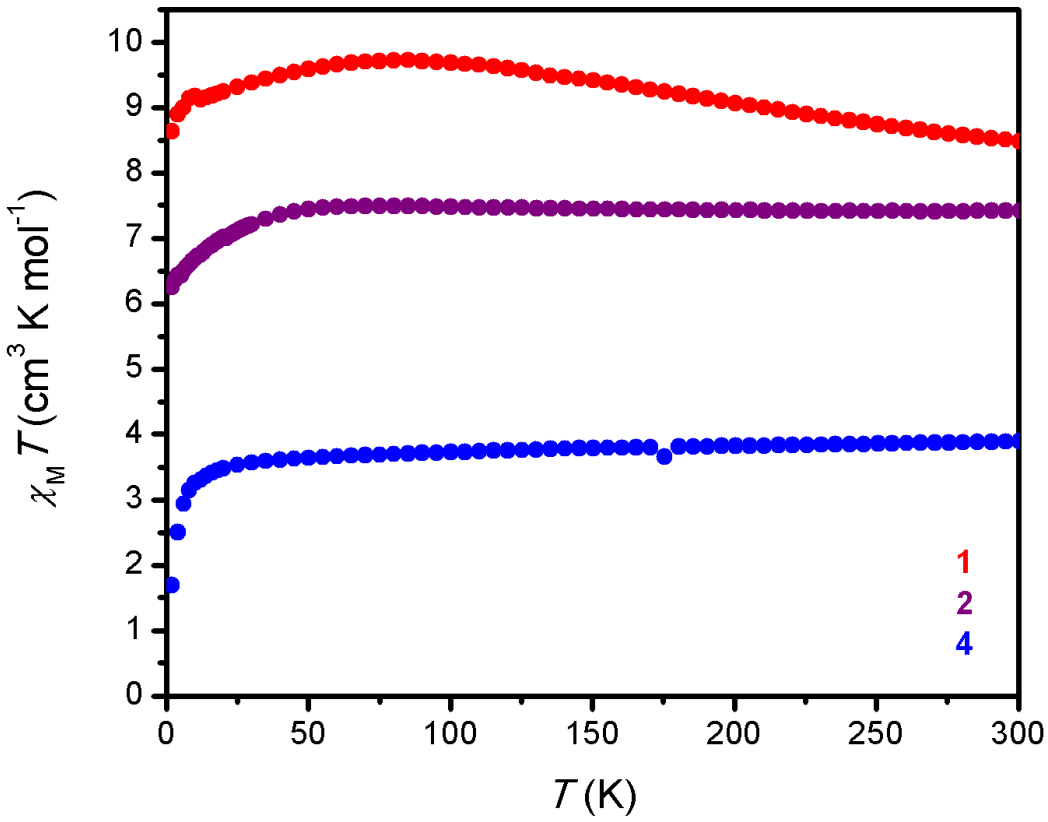

Figure S-10. Variable-temperature molar magnetic susceptibility times temperature ($\chi_M T$) for [L^{Me}Fe(μ-N_2)FeL^{Me}] (**1**) (red), [L^{Me}Fe(μ-N_2)FeL^{Me}][K(18-crown-6)(THF)$_2$] (**2**) (purple), and K_2[L^{Me}Fe(μ-N_2)FeL^{Me}] (**4**), (blue). All data were collected under an applied field of 1000 Oe.

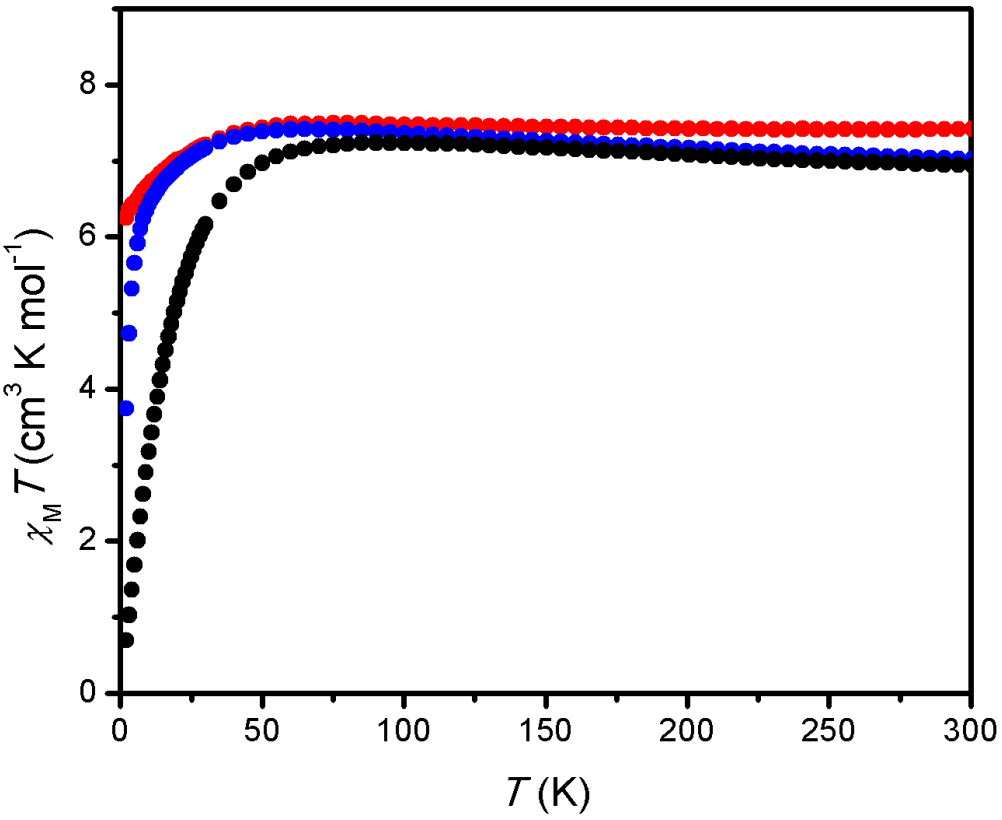

Figure S-11. Variable-temperature molar magnetic susceptibility times temperature ($\chi_M T$) for [L^{Me}Fe(μ-N_2)FeL^{Me}][K(18-crown-6)(THF)$_2$] (**2**) under applied fields of 0.1 T (red), 1 T (blue), and 7 T (black).

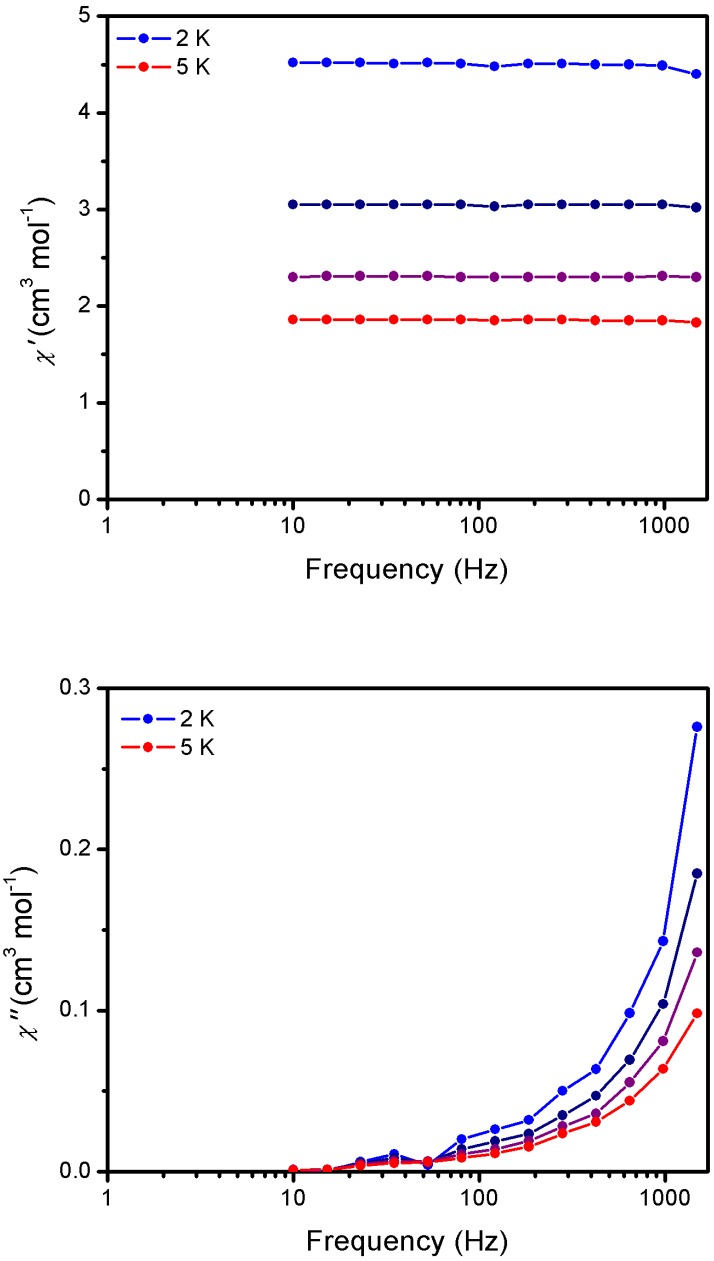

Figure S-12. In-phase (χ') and out-of-phase (χ'') magnetic susceptibility for [$L^{Me}Fe(\mu\text{-}N_2)FeL^{Me}$] (**1**) collected under zero applied dc field from 2 to 5 K. The lines are a guide for the eye.

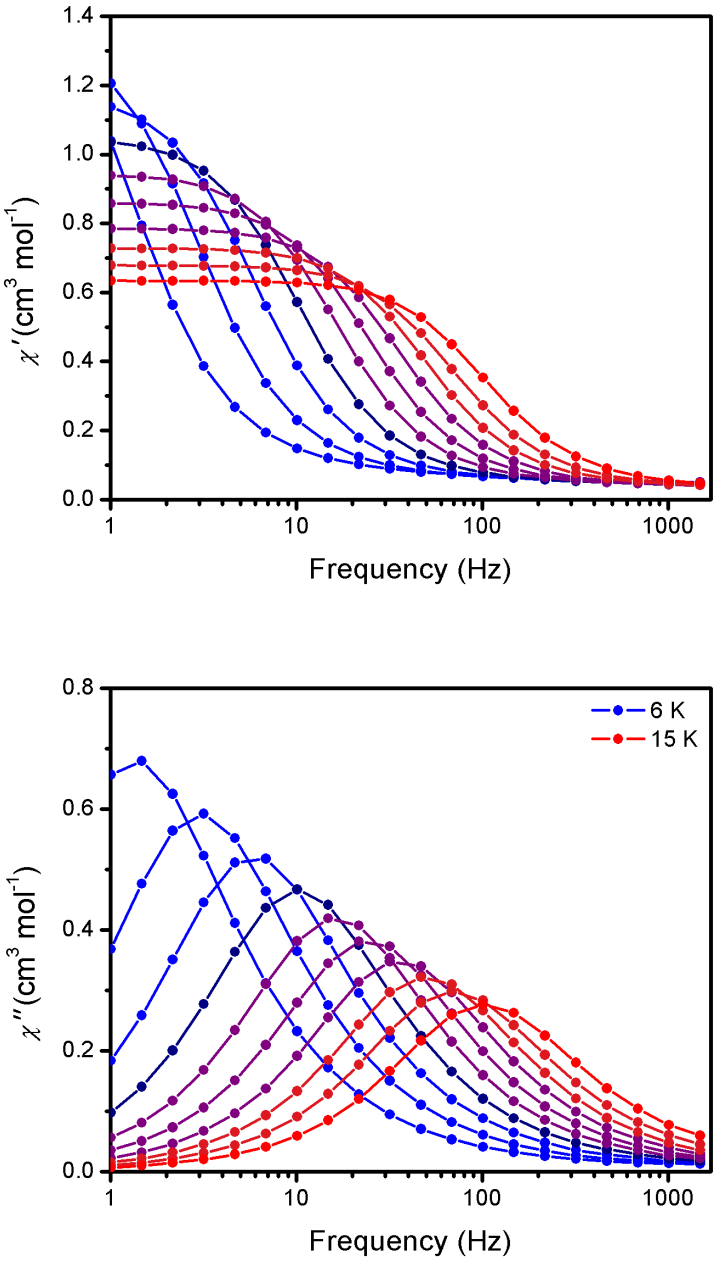

Figure S-13. In-phase (χ') and out-of-phase (χ'') magnetic susceptibility for [$L^{Me}Fe(\mu\text{-}N_2)FeL^{Me}$] (**1**) collected under a 500 Oe dc field from 6 to 15 K. The lines are a guide for the eye.

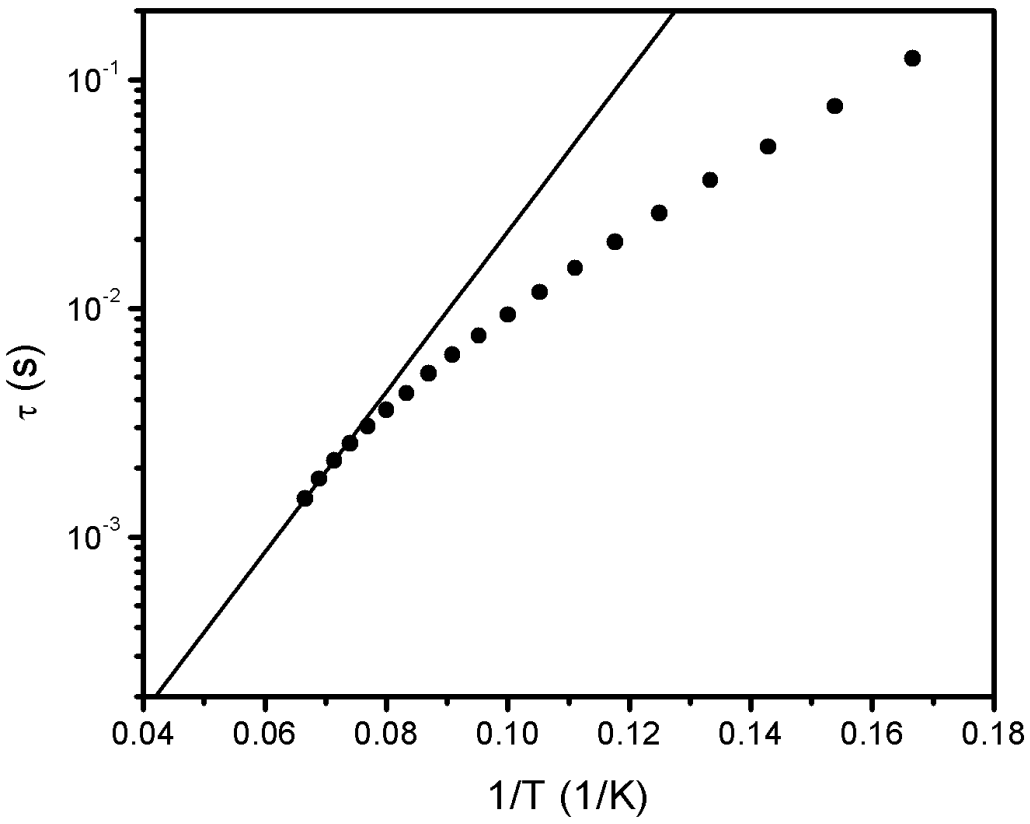

Figure S-14. Arrhenius plot for [L^{Me}Fe(μ-N_2)FeL^{Me}] (**1**) with data collected under a 500 Oe applied dc field. The line depicts the temperature dependence for an Orbach relaxation process with U_{eff} = 56.1 cm^{-1} and $\tau_0 = 6.8\times10^{-6}$ s.

Orbach relaxation processes were modeled in all Arrhenius plots using $\tau = \tau_0 \exp(U_{eff} / k_B T)$, where τ is the relaxation time, τ_0 is the attempt time, and U_{eff} is the effective spin-reversal barrier. Large values of τ_0 ($>10^{-7}$ s) likely indicate that the complex is not relaxing exclusively through an Orbach mechanism and that through-barrier processes are still contributing. As such, the values given for U_{eff} and τ_0 are lower and upper limits, respectively.

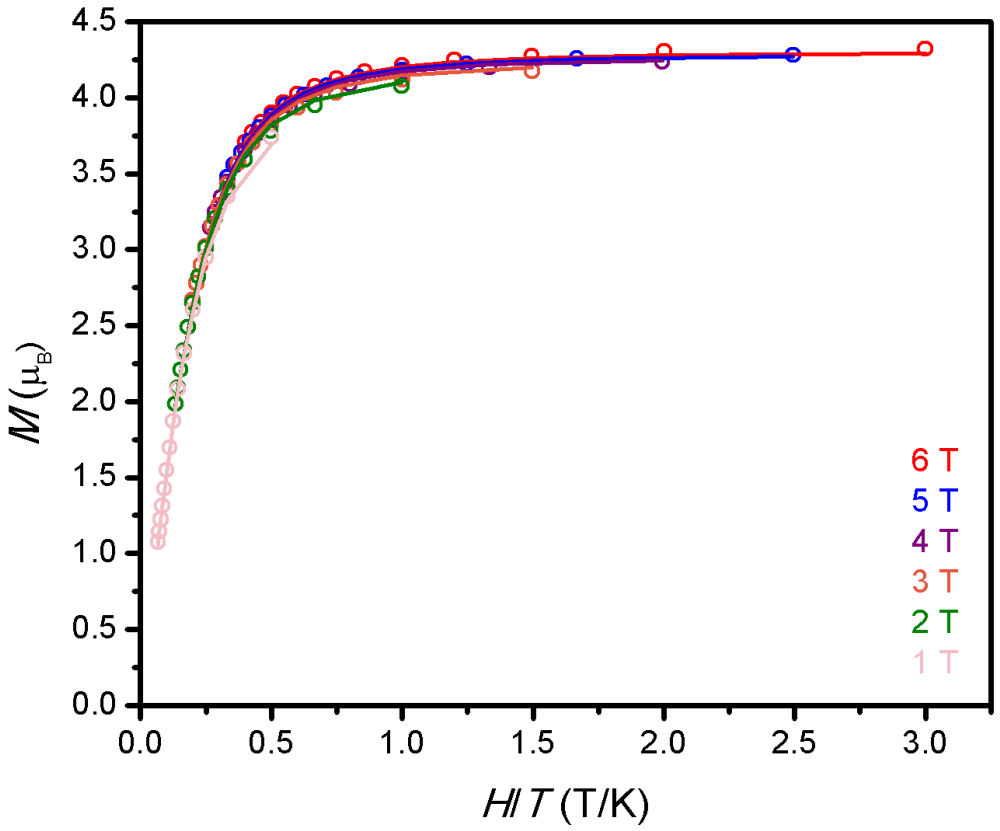

Figure S-15. Reduced magnetization data for [$L^{Me}Fe(\mu\text{-}N_2)FeL^{Me}$] (**1**) collected at temperatures from 2 to 15 K under dc fields of 1-6 T; solid lines fits using the parameters: $D = -45.0$ cm^{-1}, $|E/D| = -10.8$ cm^{-1}, $g_{\parallel} = 2.86$, $g_{\perp} = 1.40$.

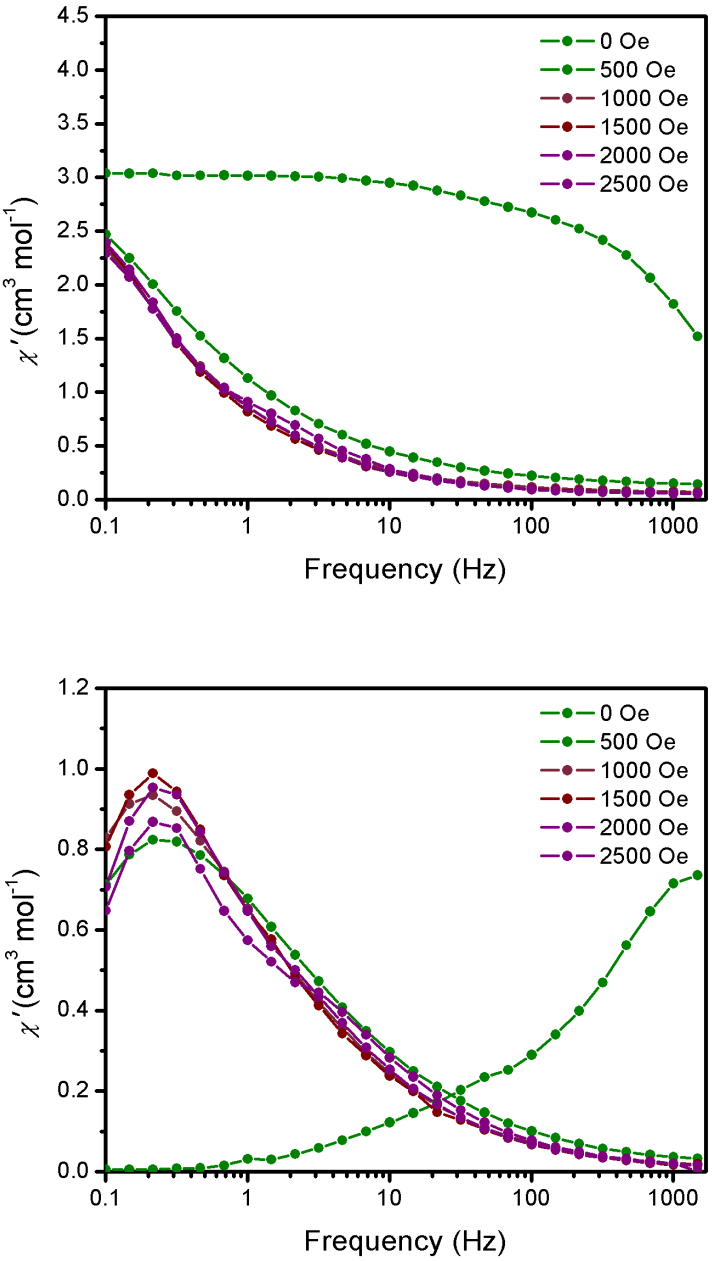

Figure S-16. In-phase (χ') and out-of-phase (χ'') magnetic susceptibility for [$L^{Me}Fe(\mu\text{-}N_2)FeL^{Me}$][K(18-crown-6)$(THF)_2$] (**2**) collected at 2 K under applied dc fields of 0-2500 Oe. The lines are a guide for the eye.

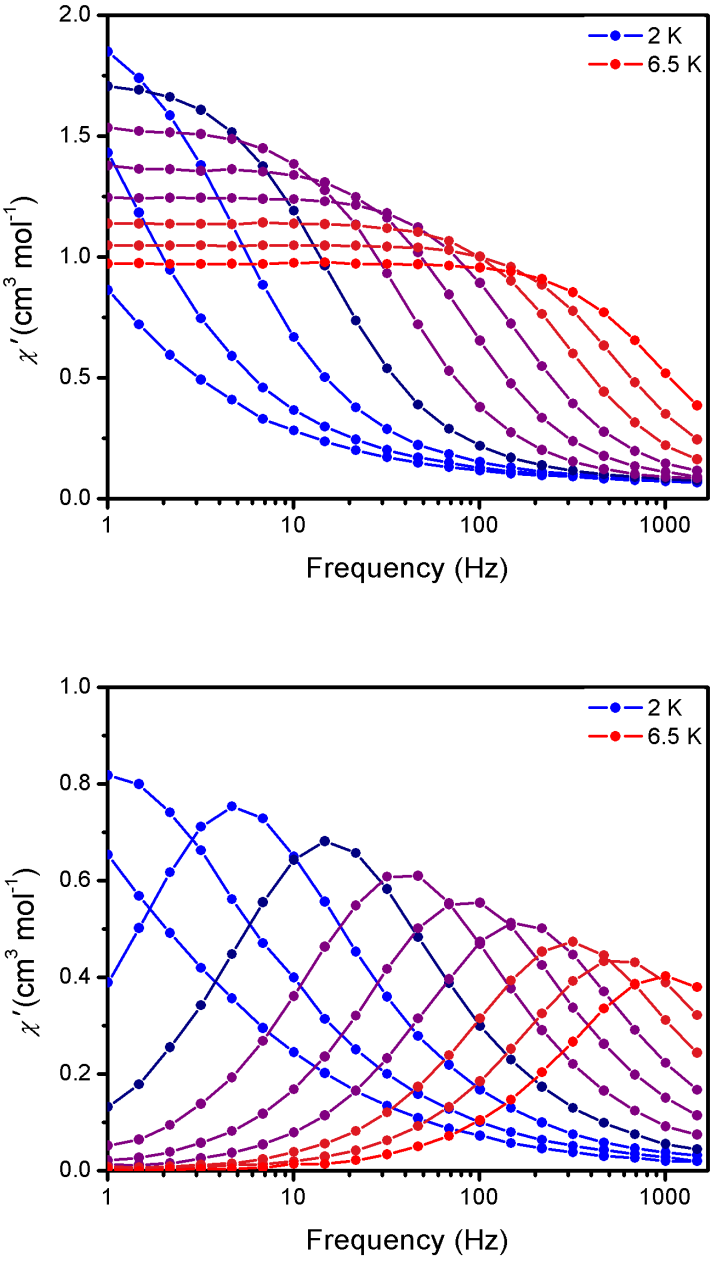

Figure S-17. In-phase (χ') and out-of-phase (χ'') magnetic susceptibility for [$L^{Me}Fe(\mu\text{-}N_2)FeL^{Me}$][K(18-crown-6)$(THF)_2$] (**2**) collected under a 1000 Oe dc field from 2 to 6.5 K. The lines are a guide for the eye.

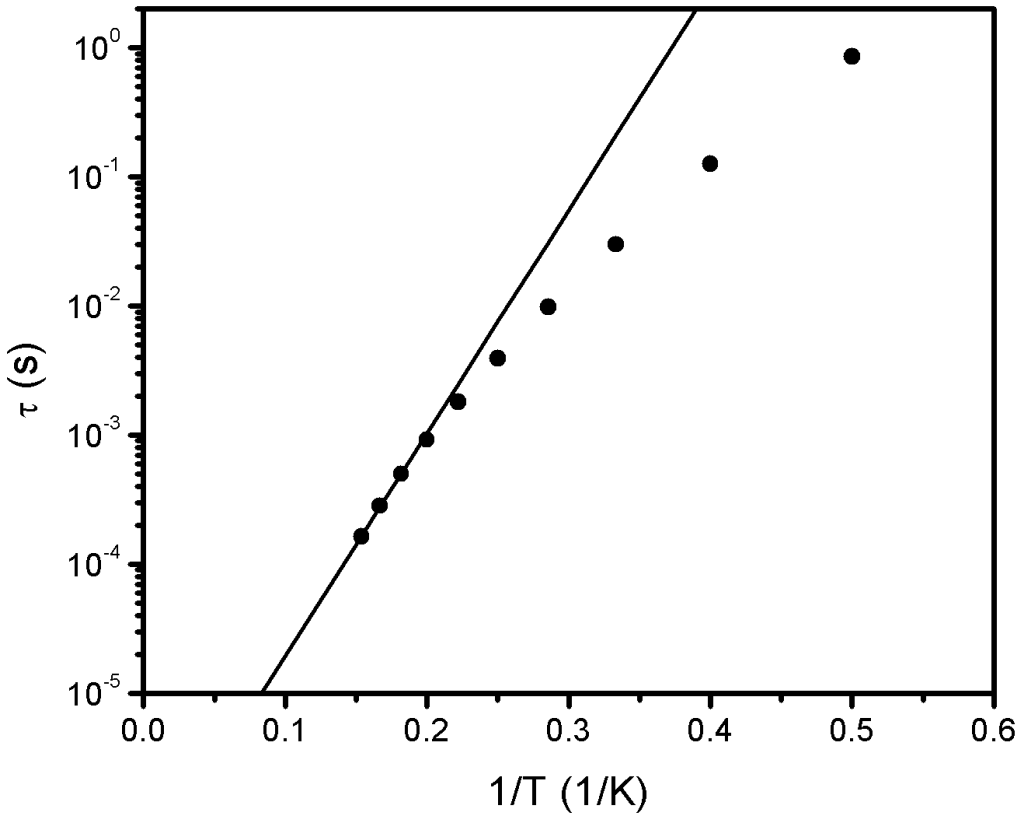

Figure S-18. Arrhenius plot for [L^{Me}Fe(μ-N_2)FeL^{Me}][K(18-crown-6)(THF)$_2$] (**2**) with data collected under a 1000 Oe applied dc field. The line depicts the temperature dependence for an Orbach relaxation process with U_{eff} = 27.6 cm^{-1} and $\tau_0 = 3.6\times10^{-7}$ s.

Orbach relaxation processes were modeled in all Arrhenius plots using $\tau = \tau_0 \exp(U_{eff} / k_B T)$, where τ is the relaxation time, τ_0 is the attempt time, and U_{eff} is the effective spin-reversal barrier. Large values of τ_0 (>10^{-7} s) likely indicate that the complex is not relaxing exclusively through an Orbach mechanism and that through-barrier processes are still contributing. As such, the values given for U_{eff} and τ_0 are lower and upper limits, respectively.

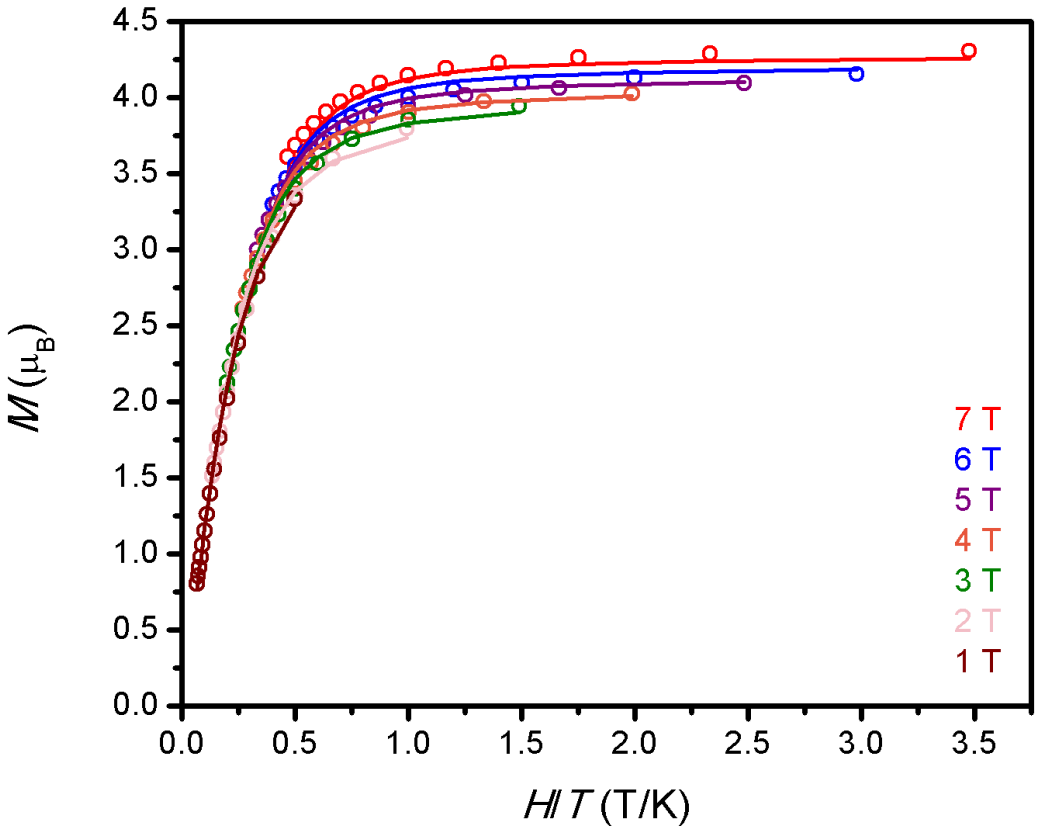

Figure S-19. Reduced magnetization data for [L^{Me}Fe(μ-N_2)FeL^{Me}][K(18-crown-6)$(THF)_2$] (**2**) collected at temperatures from 2 to 15 K under dc fields of 1-7 T. Solid lines are fits using the parameters: D = −4.5 cm^{-1}, $|E/D|$ = 0.29, $g_{//}$ = 2.96, $g_{\perp}$ = 1.51.

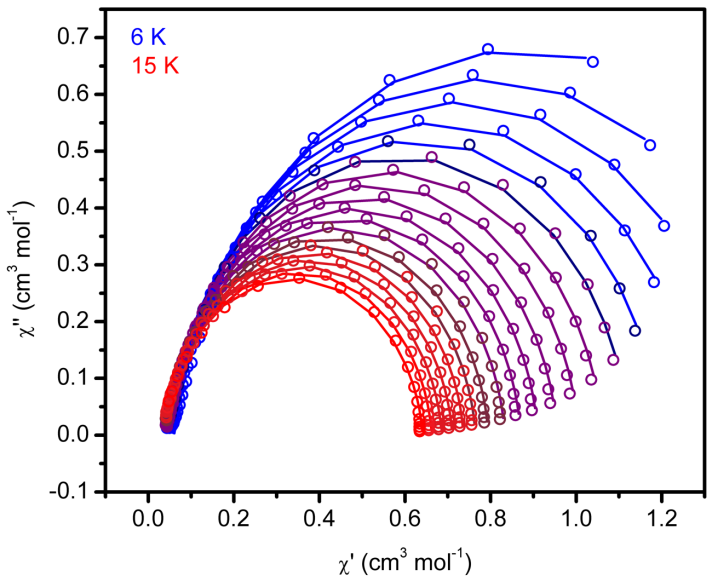

Figure S-20. Cole-Cole plot for ac magnetic susceptibility for **1**.

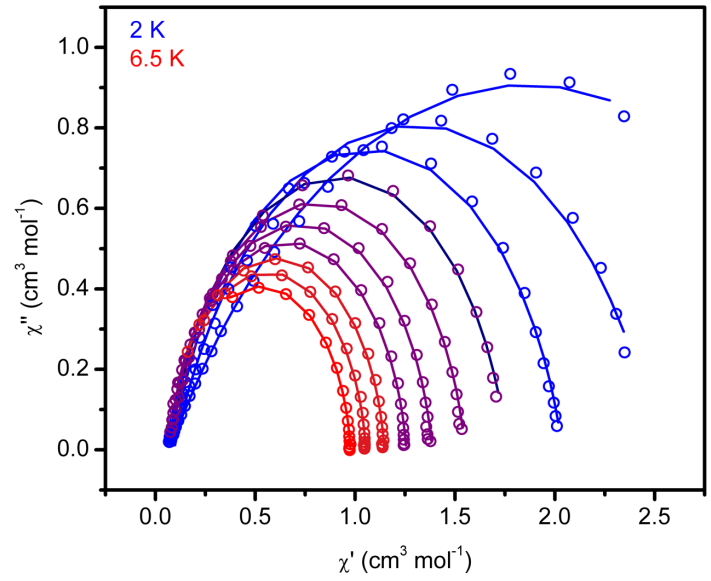

Figure S-21. Cole-Cole plot for ac magnetic susceptibility for **2**.

Additional information on relaxation fitting

In single-molecule magnetism literature since 2010,[7] relaxation data have been fit to a model originally developed by Orbach[8] and others[9] in which relaxation is attributed to a combination of relaxation mechanisms using the equation:

$$\tau^{-1} = AH^{m}T + CT^{n} + \tau_0^{-1}\exp\left(-\frac{U_{eff}}{k_B T}\right)$$

where the three terms represent direct, Raman, and Orbach relaxation, respectively, H is the applied field, τ_0 is the attempt time, and U_{eff} is the thermal barrier to spin reversal. The relaxation data for **1** and **2** can be fit solely with the Raman term (Table S1), as shown in Figures S23 and S24. We have included these fits so these data can be compared to previous analyses. Data were fit by minimizing the sum of the squares of the errors in the natural log vs. inverse temperature plot; as such the standard error of the estimate (σ_{est}) is given in terms of ln(τ).

More recent work in single-molecule magnetism, however, has explained the breakdown of the assumptions in Orbach's model, and proposed a new model that addresses these shortcomings.[10] Accurate fitting of the relaxation data within this new model requires knowledge of the low energy phonon spectrum for the system and the spin-phonon coupling terms of each phonon. As this analysis is not trivial, we have opted to simply give lower and upper limits for U_{eff} and τ_0, respectively.

Table S-1. Parameters for the relaxation data of **1** and **2** fit by Raman relaxation.

	C (s^{-1} K^{-n})	n	σ_{est}(ln τ)
1	2.3×10^{-3}	4.6	7.2×10^{-2}
2	1.1×10^{-2}	7.1	1.4×10^{-1}

Table S-2. Fits of low temperature magnetization data of **1** obtained using the program PHI.

D (cm^{-1})	$\lvert E/D\rvert$	$g_{//}$	$g_{\perp}$	Residual ($\times10^{-2}$)
-45.0	0.24	2.86	1.40	2.76
-63.2	0.21	2.85	1.68	2.76
-47.5	0.22	2.83	2.00	3.64
-38.1	0.22	2.82	1.90	4.36
-19.8	0.025	2.80	1.36	5.96
-35.5	0.077	2.80	1.80	5.96
-45.3	0.069	2.80	2.02	5.97
-43.7	0.013	2.80	2.00	5.97

Table S-3. Fits of low temperature magnetization data of **2** obtained using the program PHI.

D (cm^{-1})	$\lvert E/D\rvert$	$g_{//}$	$g_{\perp}$	Residual ($\times10^{-2}$)
-4.5	0.29	2.96	1.51	25.7

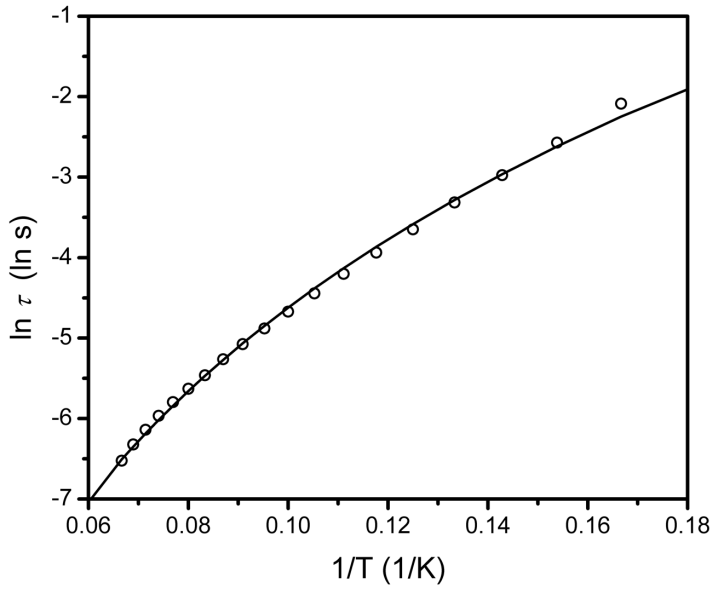

Figure S-22. Arrhenius plot of the magnetic relaxation times of **1** with a fit (solid line) using only Raman relaxation.

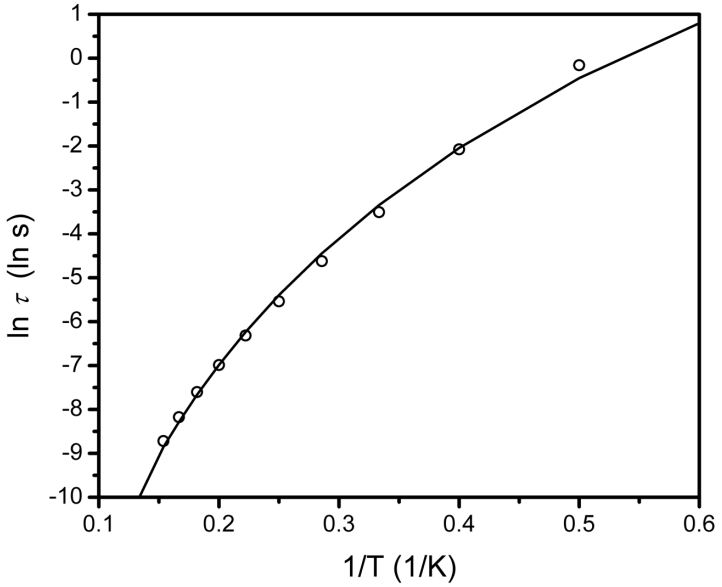

Figure S-23. Arrhenius plot of the magnetic relaxation times of **2** with a fit (solid line) using only Raman relaxation.

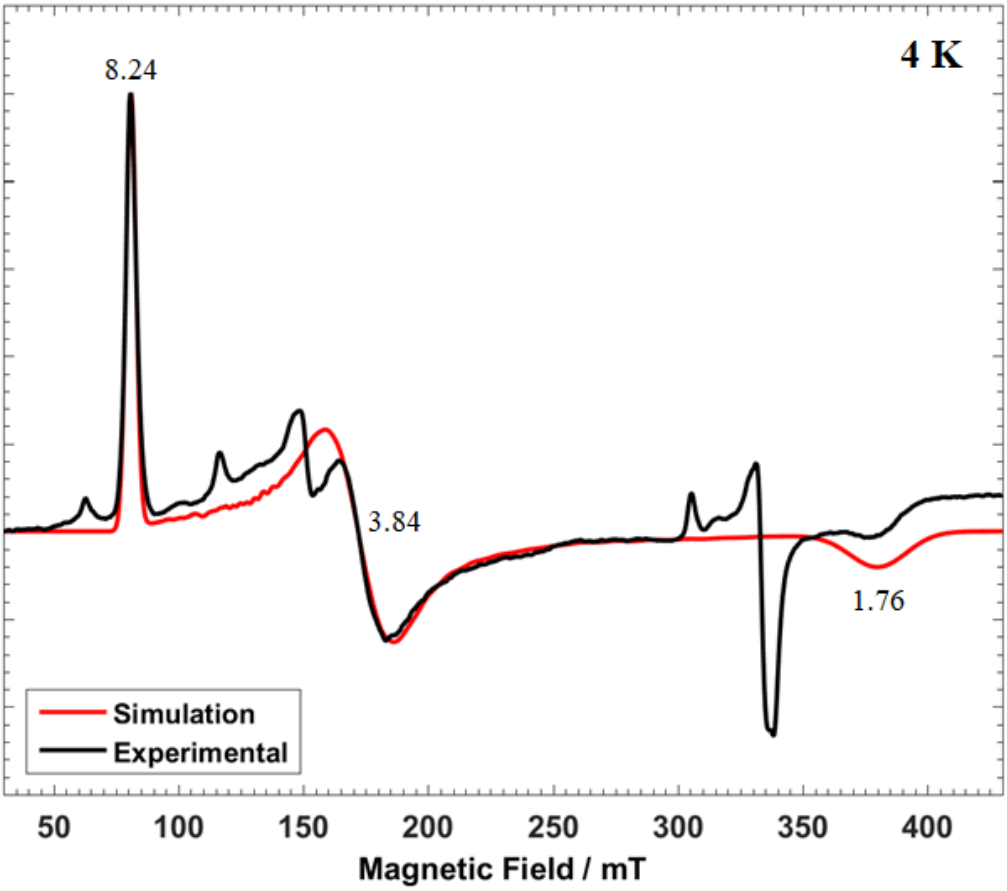

Figure S-24. Derivative X-band EPR spectra of 2 mM samples of **2** in a 1:1 mixture of THF and 2-methylTHF at 4 K (microwave frequency, 9.3734 GHz; power, 30 mW; modulation amplitude, 10 G). The spectra show the presence of several signals from the '$m_s = \pm 1/2$' ground state doublet of a $S = 5/2$ spin state with a positive D, with $D >> h\nu$ (microwave quantum). The dominant signal with effective g-values, **g'** = 8.24, 3.84, 1.76 comes from centers with $E/D = 0.097$ as demonstrated in the EasySpin simulation (simulation parameters: lw = 2.6 MHz, **g** = [2.07, 2.07, 2.04] , $D = +6.2$ cm^{-1}, $E = 0.6014$, *DStrain* = [8000; 4500] MHz).[11] In addition there is a minority $S = ½$ impurity signal in the range 300-350 mT.

Crystallography of 2. Low-temperature diffraction data (ω-scans) were collected on a Rigaku MicroMax-007HF diffractometer coupled to a Saturn994+ CCD detector with Cu Kα (λ = 1.54178 Å) for the structure of 007b-18084. The diffraction images were processed and scaled using Rigaku Oxford Diffraction software (CrysAlisPro; Rigaku: The Woodlands, TX, 2015). The structure was solved with SHELXT and was refined against F^2 on all data by full-matrix least squares with SHELXL.[12] All non-hydrogen atoms were refined anisotropically. Hydrogen atoms were included in the model at geometrically calculated positions and refined using a riding model. The isotropic displacement parameters of all hydrogen atoms were fixed to 1.2 times the U value of the atoms to which they are linked (1.5 times for methyl groups). The full numbering scheme of **2** can be found in the CIF. The structure has been deposited with the CCSD with accession code 1866500.

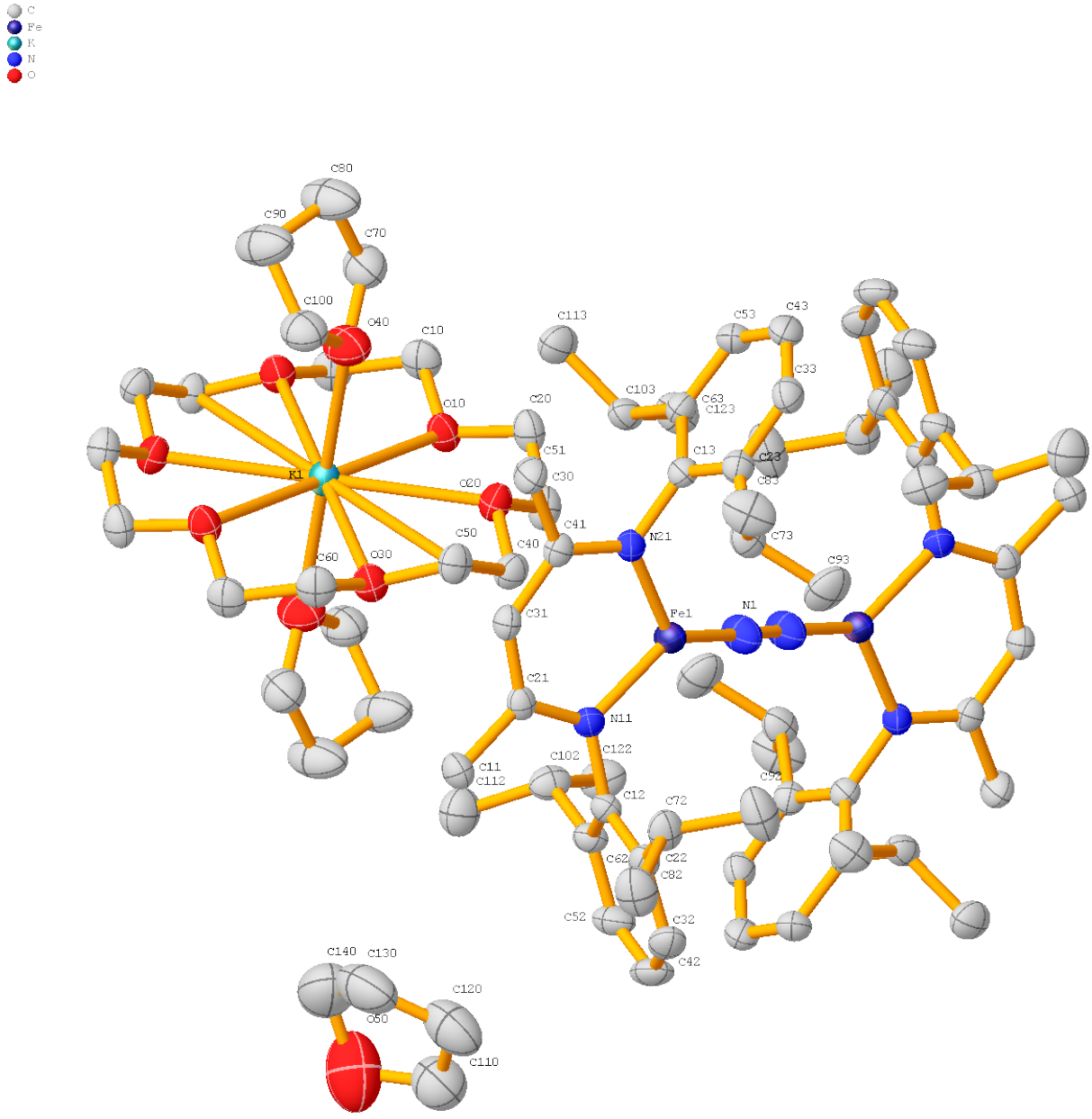

Figure S-25. The complete numbering scheme of **2** with 50% thermal ellipsoid probability levels. The hydrogen atoms are shown as circles for clarity. The molecule lies on a crystallographic special position; the unit half is labeled above.

Table S-4. Crystal data and structure refinement for **2**.

Identification code	007b-18084	
Empirical formula	C86 H136 Fe2 K N6 O10	
Formula weight	1564.80	
Temperature	93(2) K	
Wavelength	1.54184 Å	
Crystal system	Triclinic	
Space group	P-1	
Unit cell dimensions	a = 13.1435(5) Å	α= 66.914(4)°.
	b = 13.7367(6) Å	β= 88.232(3)°.
	c = 14.6446(7) Å	γ = 68.744(4)°.
Volume	2247.66(19) $Å^3$	
Z	1	
Density (calculated)	1.156 Mg/m^3	
Absorption coefficient	3.439 mm^{-1}	
F(000)	845	
Crystal size	0.130 x 0.080 x 0.050 mm^3	
Crystal color and habit	Green Block	
Diffractometer	Rigaku Saturn 944+ CCD	
Theta range for data collection	3.309 to 66.589°.	
Index ranges	-15<=h<=15, -16<=k<=16, -17<=l<=17	
Reflections collected	78976	
Independent reflections	7822 [R(int) = 0.0614]	
Observed reflections (I > 2sigma(I))	6944	
Completeness to theta = 66.589°	98.5 %	
Absorption correction	Semi-empirical from equivalents	
Max. and min. transmission	1.00000 and 0.72604	
Solution method	SHELXT-2014/5	
Refinement method	SHELXL-2014/7	
Data / restraints / parameters	7822 / 0 / 485	
Goodness-of-fit on F^2	1.070	
Final R indices [I>2sigma(I)]	R1 = 0.0601, wR2 = 0.1587	
R indices (all data)	R1 = 0.0685, wR2 = 0.1663	
Largest diff. peak and hole	0.702 and -0.543 $e.Å^{-3}$	

Table S-5. Atomic coordinates (x 10^4) and equivalent isotropic displacement parameters ($Å^2$x 10^3) for **2**. U(eq) is defined as one third of the trace of the orthogonalized U^{ij} tensor.

	x	y	z	U(eq)
Fe(1)	4874(1)	4465(1)	8691(1)	29(1)
N(1)	4966(2)	4837(3)	9686(2)	43(1)
N(11)	5990(2)	3784(2)	7990(2)	27(1)
N(21)	3586(2)	4941(2)	7769(2)	27(1)
C(11)	6671(3)	3397(3)	6528(2)	37(1)
C(21)	5753(3)	3897(2)	7055(2)	28(1)
C(31)	4683(3)	4446(3)	6543(2)	29(1)
C(41)	3667(3)	4891(3)	6871(2)	29(1)
C(51)	2632(3)	5297(3)	6178(2)	40(1)
C(12)	7074(2)	3065(3)	8527(2)	29(1)
C(22)	7373(3)	1866(3)	8981(2)	33(1)
C(32)	8395(3)	1185(3)	9571(3)	44(1)
C(42)	9112(3)	1656(3)	9703(3)	46(1)
C(52)	8821(3)	2825(3)	9247(3)	42(1)
C(62)	7803(3)	3555(3)	8657(2)	33(1)
C(72)	6587(3)	1316(3)	8891(3)	40(1)
C(82)	7140(4)	298(3)	8604(3)	55(1)
C(92)	6098(4)	939(4)	9865(3)	61(1)
C(102)	7512(3)	4833(3)	8190(3)	39(1)
C(112)	8193(4)	5165(4)	7334(3)	56(1)
C(122)	7648(3)	5280(3)	8968(3)	47(1)
C(13)	2516(2)	5301(3)	8075(2)	28(1)
C(23)	2016(3)	4494(3)	8497(2)	31(1)
C(33)	975(3)	4852(3)	8791(2)	35(1)
C(43)	438(3)	5972(3)	8698(2)	37(1)
C(53)	952(3)	6738(3)	8318(2)	34(1)
C(63)	1985(3)	6430(3)	7998(2)	30(1)
C(73)	2625(3)	3243(3)	8695(3)	37(1)
C(83)	1938(4)	2712(4)	8392(4)	59(1)
C(93)	3095(4)	2563(3)	9804(3)	59(1)
C(103)	2522(3)	7297(3)	7592(2)	34(1)
C(113)	1868(3)	8300(3)	6605(3)	47(1)
C(123)	2688(3)	7730(3)	8362(3)	46(1)

K(1)	5000	10000	5000	30(1)
O(10)	4619(2)	10914(2)	6493(2)	36(1)
O(20)	4705(2)	8702(2)	6916(2)	34(1)
O(30)	5608(2)	7658(2)	5536(2)	35(1)
C(10)	3984(3)	12116(3)	6117(3)	43(1)
C(20)	4253(3)	10273(3)	7367(3)	41(1)
C(30)	4937(3)	9028(3)	7668(3)	41(1)
C(40)	5280(3)	7506(3)	7187(2)	36(1)
C(50)	5040(3)	7218(3)	6350(2)	37(1)
C(60)	5519(3)	7297(3)	4767(3)	40(1)
O(40)	2927(2)	10313(3)	4554(2)	58(1)
C(70)	2079(3)	11315(4)	4588(3)	57(1)
C(80)	1137(4)	11649(5)	3842(4)	82(2)
C(90)	1674(4)	11113(5)	3136(4)	82(2)
C(100)	2563(3)	10021(4)	3836(3)	57(1)
O(50)	11014(5)	1912(5)	6641(4)	126(2)
C(110)	10786(5)	1110(6)	7544(5)	85(2)
C(120)	9789(5)	952(6)	7329(5)	92(2)
C(130)	9488(5)	1610(7)	6202(5)	104(2)
C(140)	9963(7)	2527(7)	5980(6)	121(3)

Table S-6. Bond lengths [Å] and angles [°] for **2**.

Fe(1)-N(1)	1.744(3)
Fe(1)-N(11)	1.936(2)
Fe(1)-N(21)	1.940(3)
N(1)-N(1)#1	1.186(6)
N(11)-C(21)	1.350(4)
N(11)-C(12)	1.436(4)
N(21)-C(41)	1.343(4)
N(21)-C(13)	1.434(4)
C(11)-C(21)	1.509(4)
C(11)-H(11A)	0.9800
C(11)-H(11B)	0.9800
C(11)-H(11C)	0.9800
C(21)-C(31)	1.400(4)
C(31)-C(41)	1.409(4)
C(31)-H(31)	0.9500
C(41)-C(51)	1.511(4)
C(51)-H(51A)	0.9800
C(51)-H(51B)	0.9800
C(51)-H(51C)	0.9800
C(12)-C(62)	1.409(5)
C(12)-C(22)	1.413(4)
C(22)-C(32)	1.397(5)
C(22)-C(72)	1.520(5)
C(32)-C(42)	1.377(6)
C(32)-H(32)	0.9500
C(42)-C(52)	1.378(5)
C(42)-H(42)	0.9500
C(52)-C(62)	1.400(5)
C(52)-H(52)	0.9500
C(62)-C(102)	1.512(5)
C(72)-C(92)	1.523(5)
C(72)-C(82)	1.537(5)
C(72)-H(72)	1.0000
C(82)-H(82A)	0.9800
C(82)-H(82B)	0.9800
C(82)-H(82C)	0.9800

C(92)-H(92A)	0.9800
C(92)-H(92B)	0.9800
C(92)-H(92C)	0.9800
C(102)-C(122)	1.532(5)
C(102)-C(112)	1.535(5)
C(102)-H(102)	1.0000
C(112)-H(11D)	0.9800
C(112)-H(11E)	0.9800
C(112)-H(11F)	0.9800
C(122)-H(12A)	0.9800
C(122)-H(12B)	0.9800
C(122)-H(12C)	0.9800
C(13)-C(63)	1.410(4)
C(13)-C(23)	1.417(4)
C(23)-C(33)	1.393(4)
C(23)-C(73)	1.518(4)
C(33)-C(43)	1.392(5)
C(33)-H(33)	0.9500
C(43)-C(53)	1.381(5)
C(43)-H(43)	0.9500
C(53)-C(63)	1.394(4)
C(53)-H(53)	0.9500
C(63)-C(103)	1.516(4)
C(73)-C(83)	1.517(5)
C(73)-C(93)	1.531(5)
C(73)-H(73)	1.0000
C(83)-H(83A)	0.9800
C(83)-H(83B)	0.9800
C(83)-H(83C)	0.9800
C(93)-H(93A)	0.9800
C(93)-H(93B)	0.9800
C(93)-H(93C)	0.9800
C(103)-C(123)	1.520(5)
C(103)-C(113)	1.544(5)
C(103)-H(103)	1.0000
C(113)-H(11G)	0.9800
C(113)-H(11H)	0.9800
C(113)-H(11I)	0.9800

C(123)-H(12D)	0.9800
C(123)-H(12E)	0.9800
C(123)-H(12F)	0.9800
K(1)-O(40)	2.660(3)
K(1)-O(40)#2	2.660(3)
K(1)-O(20)#2	2.777(2)
K(1)-O(20)	2.777(2)
K(1)-O(30)#2	2.793(2)
K(1)-O(30)	2.793(2)
K(1)-O(10)#2	2.870(2)
K(1)-O(10)	2.870(2)
K(1)-C(50)#2	3.528(3)
K(1)-C(50)	3.528(3)
O(10)-C(20)	1.425(4)
O(10)-C(10)	1.429(4)
O(20)-C(30)	1.419(4)
O(20)-C(40)	1.427(4)
O(30)-C(60)	1.418(4)
O(30)-C(50)	1.432(4)
C(10)-C(60)#2	1.505(5)
C(10)-H(10A)	0.9900
C(10)-H(10B)	0.9900
C(20)-C(30)	1.498(5)
C(20)-H(20A)	0.9900
C(20)-H(20B)	0.9900
C(30)-H(30A)	0.9900
C(30)-H(30B)	0.9900
C(40)-C(50)	1.501(5)
C(40)-H(40A)	0.9900
C(40)-H(40B)	0.9900
C(50)-H(50)	1.0000
C(60)-C(10)#2	1.505(5)
C(60)-H(60A)	0.9900
C(60)-H(60B)	0.9900
O(40)-C(100)	1.413(5)
O(40)-C(70)	1.441(5)
C(70)-C(80)	1.488(6)
C(70)-H(70A)	0.9900

C(70)-H(70B)	0.9900
C(80)-C(90)	1.512(7)
C(80)-H(80A)	0.9900
C(80)-H(80B)	0.9900
C(90)-C(100)	1.504(6)
C(90)-H(90A)	0.9900
C(90)-H(90B)	0.9900
C(100)-H(10C)	0.9900
C(100)-H(10D)	0.9900
O(50)-C(110)	1.458(8)
O(50)-C(140)	1.467(9)
C(110)-C(120)	1.465(8)
C(110)-H(11J)	0.9900
C(110)-H(11K)	0.9900
C(120)-C(130)	1.519(9)
C(120)-H(12G)	0.9900
C(120)-H(12H)	0.9900
C(130)-C(140)	1.523(11)
C(130)-H(13A)	0.9900
C(130)-H(13B)	0.9900
C(140)-H(14A)	0.9900
C(140)-H(14B)	0.9900

N(1)-Fe(1)-N(11)	131.70(12)
N(1)-Fe(1)-N(21)	128.43(12)
N(11)-Fe(1)-N(21)	98.58(10)
N(1)#1-N(1)-Fe(1)	175.2(4)
C(21)-N(11)-C(12)	120.1(2)
C(21)-N(11)-Fe(1)	121.9(2)
C(12)-N(11)-Fe(1)	117.86(19)
C(41)-N(21)-C(13)	118.8(2)
C(41)-N(21)-Fe(1)	122.1(2)
C(13)-N(21)-Fe(1)	119.01(19)
C(21)-C(11)-H(11A)	109.5
C(21)-C(11)-H(11B)	109.5
H(11A)-C(11)-H(11B)	109.5
C(21)-C(11)-H(11C)	109.5
H(11A)-C(11)-H(11C)	109.5

H(11B)-C(11)-H(11C)	109.5
N(11)-C(21)-C(31)	123.2(3)
N(11)-C(21)-C(11)	119.3(3)
C(31)-C(21)-C(11)	117.5(3)
C(21)-C(31)-C(41)	130.2(3)
C(21)-C(31)-H(31)	114.9
C(41)-C(31)-H(31)	114.9
N(21)-C(41)-C(31)	123.0(3)
N(21)-C(41)-C(51)	119.4(3)
C(31)-C(41)-C(51)	117.5(3)
C(41)-C(51)-H(51A)	109.5
C(41)-C(51)-H(51B)	109.5
H(51A)-C(51)-H(51B)	109.5
C(41)-C(51)-H(51C)	109.5
H(51A)-C(51)-H(51C)	109.5
H(51B)-C(51)-H(51C)	109.5
C(62)-C(12)-C(22)	120.3(3)
C(62)-C(12)-N(11)	120.3(3)
C(22)-C(12)-N(11)	119.2(3)
C(32)-C(22)-C(12)	118.6(3)
C(32)-C(22)-C(72)	119.7(3)
C(12)-C(22)-C(72)	121.6(3)
C(42)-C(32)-C(22)	121.5(3)
C(42)-C(32)-H(32)	119.3
C(22)-C(32)-H(32)	119.3
C(32)-C(42)-C(52)	119.6(3)
C(32)-C(42)-H(42)	120.2
C(52)-C(42)-H(42)	120.2
C(42)-C(52)-C(62)	121.6(3)
C(42)-C(52)-H(52)	119.2
C(62)-C(52)-H(52)	119.2
C(52)-C(62)-C(12)	118.4(3)
C(52)-C(62)-C(102)	119.6(3)
C(12)-C(62)-C(102)	122.0(3)
C(22)-C(72)-C(92)	110.2(3)
C(22)-C(72)-C(82)	112.5(3)
C(92)-C(72)-C(82)	110.3(3)
C(22)-C(72)-H(72)	107.9

C(92)-C(72)-H(72)	107.9
C(82)-C(72)-H(72)	107.9
C(72)-C(82)-H(82A)	109.5
C(72)-C(82)-H(82B)	109.5
H(82A)-C(82)-H(82B)	109.5
C(72)-C(82)-H(82C)	109.5
H(82A)-C(82)-H(82C)	109.5
H(82B)-C(82)-H(82C)	109.5
C(72)-C(92)-H(92A)	109.5
C(72)-C(92)-H(92B)	109.5
H(92A)-C(92)-H(92B)	109.5
C(72)-C(92)-H(92C)	109.5
H(92A)-C(92)-H(92C)	109.5
H(92B)-C(92)-H(92C)	109.5
C(62)-C(102)-C(122)	111.8(3)
C(62)-C(102)-C(112)	111.0(3)
C(122)-C(102)-C(112)	110.8(3)
C(62)-C(102)-H(102)	107.7
C(122)-C(102)-H(102)	107.7
C(112)-C(102)-H(102)	107.7
C(102)-C(112)-H(11D)	109.5
C(102)-C(112)-H(11E)	109.5
H(11D)-C(112)-H(11E)	109.5
C(102)-C(112)-H(11F)	109.5
H(11D)-C(112)-H(11F)	109.5
H(11E)-C(112)-H(11F)	109.5
C(102)-C(122)-H(12A)	109.5
C(102)-C(122)-H(12B)	109.5
H(12A)-C(122)-H(12B)	109.5
C(102)-C(122)-H(12C)	109.5
H(12A)-C(122)-H(12C)	109.5
H(12B)-C(122)-H(12C)	109.5
C(63)-C(13)-C(23)	120.2(3)
C(63)-C(13)-N(21)	120.5(3)
C(23)-C(13)-N(21)	119.2(3)
C(33)-C(23)-C(13)	118.7(3)
C(33)-C(23)-C(73)	120.0(3)
C(13)-C(23)-C(73)	121.1(3)

C(43)-C(33)-C(23)	121.3(3)
C(43)-C(33)-H(33)	119.4
C(23)-C(33)-H(33)	119.4
C(53)-C(43)-C(33)	119.4(3)
C(53)-C(43)-H(43)	120.3
C(33)-C(43)-H(43)	120.3
C(43)-C(53)-C(63)	121.8(3)
C(43)-C(53)-H(53)	119.1
C(63)-C(53)-H(53)	119.1
C(53)-C(63)-C(13)	118.6(3)
C(53)-C(63)-C(103)	120.0(3)
C(13)-C(63)-C(103)	121.4(3)
C(83)-C(73)-C(23)	114.3(3)
C(83)-C(73)-C(93)	110.4(3)
C(23)-C(73)-C(93)	109.1(3)
C(83)-C(73)-H(73)	107.6
C(23)-C(73)-H(73)	107.6
C(93)-C(73)-H(73)	107.6
C(73)-C(83)-H(83A)	109.5
C(73)-C(83)-H(83B)	109.5
H(83A)-C(83)-H(83B)	109.5
C(73)-C(83)-H(83C)	109.5
H(83A)-C(83)-H(83C)	109.5
H(83B)-C(83)-H(83C)	109.5
C(73)-C(93)-H(93A)	109.5
C(73)-C(93)-H(93B)	109.5
H(93A)-C(93)-H(93B)	109.5
C(73)-C(93)-H(93C)	109.5
H(93A)-C(93)-H(93C)	109.5
H(93B)-C(93)-H(93C)	109.5
C(63)-C(103)-C(123)	111.6(3)
C(63)-C(103)-C(113)	111.6(3)
C(123)-C(103)-C(113)	111.0(3)
C(63)-C(103)-H(103)	107.5
C(123)-C(103)-H(103)	107.5
C(113)-C(103)-H(103)	107.5
C(103)-C(113)-H(11G)	109.5
C(103)-C(113)-H(11H)	109.5

H(11G)-C(113)-H(11H)	109.5
C(103)-C(113)-H(11I)	109.5
H(11G)-C(113)-H(11I)	109.5
H(11H)-C(113)-H(11I)	109.5
C(103)-C(123)-H(12D)	109.5
C(103)-C(123)-H(12E)	109.5
H(12D)-C(123)-H(12E)	109.5
C(103)-C(123)-H(12F)	109.5
H(12D)-C(123)-H(12F)	109.5
H(12E)-C(123)-H(12F)	109.5
O(40)-K(1)-O(40)#2	180.0
O(40)-K(1)-O(20)#2	96.69(8)
O(40)#2-K(1)-O(20)#2	83.31(8)
O(40)-K(1)-O(20)	83.31(8)
O(40)#2-K(1)-O(20)	96.69(8)
O(20)#2-K(1)-O(20)	180.0
O(40)-K(1)-O(30)#2	90.80(8)
O(40)#2-K(1)-O(30)#2	89.20(8)
O(20)#2-K(1)-O(30)#2	62.90(6)
O(20)-K(1)-O(30)#2	117.10(6)
O(40)-K(1)-O(30)	89.19(8)
O(40)#2-K(1)-O(30)	90.80(8)
O(20)#2-K(1)-O(30)	117.10(6)
O(20)-K(1)-O(30)	62.90(6)
O(30)#2-K(1)-O(30)	180.00(3)
O(40)-K(1)-O(10)#2	82.73(8)
O(40)#2-K(1)-O(10)#2	97.27(8)
O(20)#2-K(1)-O(10)#2	59.69(6)
O(20)-K(1)-O(10)#2	120.31(6)
O(30)#2-K(1)-O(10)#2	120.83(6)
O(30)-K(1)-O(10)#2	59.18(6)
O(40)-K(1)-O(10)	97.27(8)
O(40)#2-K(1)-O(10)	82.73(8)
O(20)#2-K(1)-O(10)	120.31(6)
O(20)-K(1)-O(10)	59.69(6)
O(30)#2-K(1)-O(10)	59.17(6)
O(30)-K(1)-O(10)	120.82(6)
O(10)#2-K(1)-O(10)	180.0

O(40)-K(1)-C(50)#2	101.37(9)
O(40)#2-K(1)-C(50)#2	78.63(9)
O(20)#2-K(1)-C(50)#2	42.40(7)
O(20)-K(1)-C(50)#2	137.60(7)
O(30)#2-K(1)-C(50)#2	22.57(7)
O(30)-K(1)-C(50)#2	157.43(7)
O(10)#2-K(1)-C(50)#2	102.05(7)
O(10)-K(1)-C(50)#2	77.95(7)
O(40)-K(1)-C(50)	78.63(9)
O(40)#2-K(1)-C(50)	101.37(9)
O(20)#2-K(1)-C(50)	137.60(7)
O(20)-K(1)-C(50)	42.40(7)
O(30)#2-K(1)-C(50)	157.43(7)
O(30)-K(1)-C(50)	22.57(7)
O(10)#2-K(1)-C(50)	77.95(7)
O(10)-K(1)-C(50)	102.05(7)
C(50)#2-K(1)-C(50)	180.0
C(20)-O(10)-C(10)	112.7(2)
C(20)-O(10)-K(1)	114.52(18)
C(10)-O(10)-K(1)	114.58(19)
C(30)-O(20)-C(40)	111.4(2)
C(30)-O(20)-K(1)	114.76(18)
C(40)-O(20)-K(1)	111.74(18)
C(60)-O(30)-C(50)	111.4(2)
C(60)-O(30)-K(1)	117.78(18)
C(50)-O(30)-K(1)	108.94(17)
O(10)-C(10)-C(60)#2	107.8(3)
O(10)-C(10)-H(10A)	110.2
C(60)#2-C(10)-H(10A)	110.2
O(10)-C(10)-H(10B)	110.2
C(60)#2-C(10)-H(10B)	110.2
H(10A)-C(10)-H(10B)	108.5
O(10)-C(20)-C(30)	108.2(3)
O(10)-C(20)-H(20A)	110.1
C(30)-C(20)-H(20A)	110.1
O(10)-C(20)-H(20B)	110.1
C(30)-C(20)-H(20B)	110.1
H(20A)-C(20)-H(20B)	108.4

O(20)-C(30)-C(20)	108.5(3)
O(20)-C(30)-H(30A)	110.0
C(20)-C(30)-H(30A)	110.0
O(20)-C(30)-H(30B)	110.0
C(20)-C(30)-H(30B)	110.0
H(30A)-C(30)-H(30B)	108.4
O(20)-C(40)-C(50)	109.1(3)
O(20)-C(40)-H(40A)	109.9
C(50)-C(40)-H(40A)	109.9
O(20)-C(40)-H(40B)	109.9
C(50)-C(40)-H(40B)	109.9
H(40A)-C(40)-H(40B)	108.3
O(30)-C(50)-C(40)	108.7(3)
O(30)-C(50)-K(1)	48.49(13)
C(40)-C(50)-K(1)	79.02(17)
O(30)-C(50)-H(50)	124.5
C(40)-C(50)-H(50)	124.5
K(1)-C(50)-H(50)	124.5
O(30)-C(60)-C(10)#2	109.4(3)
O(30)-C(60)-H(60A)	109.8
C(10)#2-C(60)-H(60A)	109.8
O(30)-C(60)-H(60B)	109.8
C(10)#2-C(60)-H(60B)	109.8
H(60A)-C(60)-H(60B)	108.2
C(100)-O(40)-C(70)	109.7(3)
C(100)-O(40)-K(1)	125.1(2)
C(70)-O(40)-K(1)	117.0(2)
O(40)-C(70)-C(80)	106.5(4)
O(40)-C(70)-H(70A)	110.4
C(80)-C(70)-H(70A)	110.4
O(40)-C(70)-H(70B)	110.4
C(80)-C(70)-H(70B)	110.4
H(70A)-C(70)-H(70B)	108.6
C(70)-C(80)-C(90)	103.1(4)
C(70)-C(80)-H(80A)	111.1
C(90)-C(80)-H(80A)	111.1
C(70)-C(80)-H(80B)	111.1
C(90)-C(80)-H(80B)	111.1

H(80A)-C(80)-H(80B)	109.1
C(100)-C(90)-C(80)	101.9(4)
C(100)-C(90)-H(90A)	111.4
C(80)-C(90)-H(90A)	111.4
C(100)-C(90)-H(90B)	111.4
C(80)-C(90)-H(90B)	111.4
H(90A)-C(90)-H(90B)	109.3
O(40)-C(100)-C(90)	104.8(4)
O(40)-C(100)-H(10C)	110.8
C(90)-C(100)-H(10C)	110.8
O(40)-C(100)-H(10D)	110.8
C(90)-C(100)-H(10D)	110.8
H(10C)-C(100)-H(10D)	108.9
C(110)-O(50)-C(140)	104.2(5)
O(50)-C(110)-C(120)	110.2(5)
O(50)-C(110)-H(11J)	109.6
C(120)-C(110)-H(11J)	109.6
O(50)-C(110)-H(11K)	109.6
C(120)-C(110)-H(11K)	109.6
H(11J)-C(110)-H(11K)	108.1
C(110)-C(120)-C(130)	104.1(6)
C(110)-C(120)-H(12G)	110.9
C(130)-C(120)-H(12G)	110.9
C(110)-C(120)-H(12H)	110.9
C(130)-C(120)-H(12H)	110.9
H(12G)-C(120)-H(12H)	108.9
C(120)-C(130)-C(140)	102.3(6)
C(120)-C(130)-H(13A)	111.3
C(140)-C(130)-H(13A)	111.3
C(120)-C(130)-H(13B)	111.3
C(140)-C(130)-H(13B)	111.3
H(13A)-C(130)-H(13B)	109.2
O(50)-C(140)-C(130)	103.3(6)
O(50)-C(140)-H(14A)	111.1
C(130)-C(140)-H(14A)	111.1
O(50)-C(140)-H(14B)	111.1
C(130)-C(140)-H(14B)	111.1
H(14A)-C(140)-H(14B)	109.1

Table S-7. Anisotropic displacement parameters ($Å^2 x\ 10^3$) for **2**. The anisotropic displacement factor exponent takes the form: $-2\pi^2[\ h^2\ a^{*2}U^{11} + ...\ + 2\ h\ k\ a^*\ b^*\ U^{12}\ ]$

	U^{11}	U^{22}	U^{33}	U^{23}	U^{13}	U^{12}
Fe(1)	29(1)	30(1)	28(1)	-14(1)	3(1)	-8(1)
N(1)	39(2)	56(2)	42(2)	-32(1)	5(1)	-15(1)
N(11)	27(1)	24(1)	28(1)	-10(1)	3(1)	-8(1)
N(21)	29(1)	26(1)	25(1)	-10(1)	5(1)	-11(1)
C(11)	36(2)	42(2)	32(2)	-18(2)	10(1)	-13(2)
C(21)	35(2)	24(1)	26(2)	-11(1)	9(1)	-14(1)
C(31)	35(2)	31(2)	23(1)	-11(1)	5(1)	-14(1)
C(41)	34(2)	27(2)	26(2)	-8(1)	4(1)	-13(1)
C(51)	37(2)	51(2)	29(2)	-15(2)	1(1)	-14(2)
C(12)	27(2)	29(2)	28(2)	-14(1)	6(1)	-6(1)
C(22)	39(2)	28(2)	28(2)	-12(1)	7(1)	-6(1)
C(32)	45(2)	30(2)	38(2)	-13(2)	5(2)	3(2)
C(42)	32(2)	43(2)	48(2)	-21(2)	-3(2)	7(2)
C(52)	28(2)	45(2)	50(2)	-23(2)	1(2)	-4(2)
C(62)	27(2)	32(2)	35(2)	-15(1)	4(1)	-6(1)
C(72)	53(2)	29(2)	39(2)	-13(1)	12(2)	-16(2)
C(82)	73(3)	44(2)	58(2)	-29(2)	21(2)	-26(2)
C(92)	82(3)	58(3)	62(3)	-33(2)	37(2)	-39(2)
C(102)	34(2)	33(2)	47(2)	-14(2)	-1(2)	-13(1)
C(112)	66(3)	52(2)	51(2)	-16(2)	11(2)	-28(2)
C(122)	49(2)	40(2)	54(2)	-21(2)	-2(2)	-15(2)
C(13)	26(2)	30(2)	24(1)	-10(1)	1(1)	-9(1)
C(23)	32(2)	32(2)	29(2)	-12(1)	4(1)	-13(1)
C(33)	33(2)	40(2)	31(2)	-12(1)	7(1)	-17(1)
C(43)	26(2)	43(2)	36(2)	-11(2)	4(1)	-12(1)
C(53)	29(2)	31(2)	35(2)	-12(1)	4(1)	-6(1)
C(63)	30(2)	28(2)	27(2)	-6(1)	2(1)	-10(1)
C(73)	38(2)	32(2)	43(2)	-15(2)	12(2)	-17(1)
C(83)	56(2)	57(2)	83(3)	-43(2)	12(2)	-27(2)
C(93)	76(3)	29(2)	52(2)	-8(2)	-4(2)	-9(2)
C(103)	31(2)	26(2)	40(2)	-10(1)	8(1)	-9(1)
C(113)	46(2)	33(2)	48(2)	-5(2)	7(2)	-14(2)
C(123)	47(2)	41(2)	58(2)	-24(2)	13(2)	-22(2)

K(1)	36(1)	27(1)	29(1)	-12(1)	6(1)	-12(1)
O(10)	43(1)	35(1)	36(1)	-18(1)	13(1)	-16(1)
O(20)	44(1)	30(1)	28(1)	-10(1)	4(1)	-15(1)
O(30)	41(1)	30(1)	37(1)	-16(1)	9(1)	-16(1)
C(10)	51(2)	35(2)	46(2)	-24(2)	12(2)	-13(2)
C(20)	53(2)	44(2)	33(2)	-20(2)	16(2)	-22(2)
C(30)	53(2)	44(2)	31(2)	-14(2)	7(2)	-24(2)
C(40)	40(2)	30(2)	33(2)	-7(1)	3(1)	-13(1)
C(50)	45(2)	32(2)	35(2)	-10(1)	8(1)	-21(2)
C(60)	51(2)	31(2)	45(2)	-21(2)	9(2)	-17(2)
O(40)	41(1)	75(2)	57(2)	-31(2)	-2(1)	-15(1)
C(70)	52(2)	70(3)	51(2)	-28(2)	4(2)	-21(2)
C(80)	53(3)	111(4)	78(3)	-62(3)	-11(2)	0(3)
C(90)	64(3)	96(4)	68(3)	-50(3)	-15(2)	9(3)
C(100)	45(2)	68(3)	57(2)	-29(2)	1(2)	-16(2)
O(50)	162(5)	159(5)	94(3)	-62(3)	39(3)	-90(4)
C(110)	78(4)	95(4)	84(4)	-42(3)	13(3)	-31(3)
C(120)	75(4)	122(5)	102(5)	-72(4)	30(3)	-35(3)
C(130)	65(3)	147(6)	98(5)	-76(5)	13(3)	-9(4)
C(140)	113(6)	100(5)	93(5)	-27(4)	16(4)	6(5)

Table S-8. Hydrogen coordinates (x 10^4) and isotropic displacement parameters ($Å^2$x 10^3) for **2**.

	x	y	z	U(eq)
H(11A)	7262	3667	6547	55
H(11B)	6387	3640	5831	55
H(11C)	6959	2560	6865	55
H(31)	4634	4531	5868	35
H(51A)	2210	4819	6492	60
H(51B)	2829	5239	5545	60
H(51C)	2184	6095	6048	60
H(32)	8599	379	9889	52
H(42)	9804	1178	10105	56
H(52)	9323	3144	9335	51
H(72)	5970	1906	8351	48
H(82A)	7470	546	7987	82
H(82B)	6588	16	8497	82
H(82C)	7715	-315	9145	82
H(92A)	6687	352	10405	92
H(92B)	5562	625	9786	92
H(92C)	5730	1599	10030	92
H(102)	6720	5211	7897	47
H(11D)	8976	4814	7601	84
H(11E)	7962	5999	7019	84
H(11F)	8078	4892	6835	84
H(12A)	7181	5090	9490	71
H(12B)	7429	6112	8642	71
H(12C)	8419	4923	9269	71
H(33)	625	4323	9059	42
H(43)	-276	6207	8893	45
H(53)	592	7495	8275	41
H(73)	3261	3191	8298	44
H(83A)	1340	2696	8807	88
H(83B)	2403	1930	8487	88
H(83C)	1627	3168	7686	88
H(93A)	3569	2890	9980	88

H(93B)	3527	1762	9928	88
H(93C)	2490	2600	10214	88
H(103)	3267	6898	7440	41
H(11G)	1813	8004	6107	70
H(11H)	2247	8832	6354	70
H(11I)	1127	8702	6726	70
H(12D)	1974	8084	8558	69
H(12E)	3023	8298	8072	69
H(12F)	3173	7088	8953	69
H(10A)	3999	12397	6642	51
H(10B)	3209	12277	5911	51
H(20A)	3466	10421	7226	49
H(20B)	4334	10500	7915	49
H(30A)	5729	8894	7743	49
H(30B)	4761	8567	8318	49
H(40A)	5041	7064	7807	44
H(40B)	6081	7302	7315	44
H(50)	4422	6977	6292	44
H(60A)	4735	7490	4563	49
H(60B)	5910	6457	5017	49
H(70A)	2349	11943	4416	69
H(70B)	1852	11141	5266	69
H(80A)	779	12492	3487	98
H(80B)	583	11342	4166	98
H(90A)	1146	10957	2801	99
H(90B)	1988	11607	2622	99
H(10C)	2267	9417	4159	68
H(10D)	3173	9747	3473	68
H(11J)	10685	1407	8070	102
H(11K)	11417	365	7794	102
H(12G)	9191	1266	7684	110
H(12H)	9937	131	7530	110
H(13A)	8680	1955	6011	125
H(13B)	9829	1111	5848	125
H(14A)	10080	2835	5269	145
H(14B)	9473	3165	6140	145

References for Supporting Information:

(1) M. S. Dresselhaus and G. Dresselhaus, *Adv. Phys.,* 1981, **30**, 139.

(2) J. M. Smith, A. R. Sadique, T. R. Cundari, K. R. Rodgers, G. Lukat-Rodgers, R. J. Lachicotte, C. J. Flaschenriem, J. Vela and P. L. Holland, *J. Am. Chem. Soc.*, 2006, **128**, 756.

(3) J. M. Smith, R. J. Lachicotte, K. A. Pittard, T. R. Cundari, G. Lukat-Rodgers, K. R. Rodgers and P. L. Holland, *J. Am. Chem. Soc.*, 2001, **123**, 9222.

(4) E. M. Schubert, *J. Chem. Educ.* 1992, **69**, 62.

(5) K. S. Cole and R. H. Cole. *J. Chem. Phys.* 1941, **9**, 341.

(6) N. F. Chilton, R. P. Anderson, L. D. Turner, A. Soncini and K. S. Murray, *J. Comput. Chem.* 2013, **34**, 1164.

(7) W. H. Harman, T. D. Harris, D. E. Freedman, H. Fong, A. Chang, J. D. Rinehart, A. Ozarowski, M. T. Sougrati, F. Grandjean, G. J. Long, J. R. Long and C. J. Chang, *J. Am. Chem. Soc.* 2010, **132**, 18115.

(8) R. Orbach, *Proc. Phys. Soc. A*. 1961, **264**, 458.

(9) K. N. Shrivastava, *Phys. Stat. Sol. B* 1983, **117**, 437.

(10) a) A. Lunghi, F. Totti, R. Sessoli and S. Sanvito. *Nat. Commun.* 2017, **8**, 14620; b) A. Lunghi, F. Totti, S. Sanvito and R. Sessoli. *Chem. Sci.* 2017, **8**, 6051; c) L. Escalera-Moreno, J. J. Baldoví, A. Gaita-Ariño and E. Coronado. *Chem. Sci.* 2018, **9**, 3265

(11) S. Stoll, A. Schweiger, *J. Magn. Reson.* 2006, **178(1)**, 42-55.

(12) G. M. Sheldrick, *Acta Cryst.,* 2008, **A64**, 112.